Molecular Therapy
Methods & Clinical Development
Original Article

# iPSC-derived mesenchymal stem cells attenuate cerebral ischemia-reperfusion injury by inhibiting inflammatory signaling and oxidative stress

Masafumi Arakawa,[1,2,5] Yuki Sakamoto,[1,5] Yoshitaka Miyagawa,[2] Chikako Nito,[1,3] Shiro Takahashi,[1,2] Yuko Nitahara-Kasahara,[4] Satoshi Suda,[1] Yoshiyuki Yamazaki,[2] Mashito Sakai,[2] Kazumi Kimura,[1] and Takashi Okada[4]

[1]Department of Neurological Science, Graduate School of Medicine, Nippon Medical School, Tokyo, Japan; [2]Department of Biochemistry and Molecular Biology, Graduate School of Medicine, Nippon Medical School, Tokyo, Japan; [3]Laboratory for Clinical Research, Collaborative Research Center, Nippon Medical School, Tokyo, Japan; [4]Division of Molecular and Medical Genetics, The Institute of Medical Science, The University of Tokyo, Tokyo, Japan

**Induced pluripotent stem cell-derived mesenchymal stem cells (iMSCs) hold great promise as a cell source for transplantation into injured tissues to alleviate inflammation. However, the therapeutic efficacy of iMSC transplantation for ischemic stroke remains unknown. In this study, we evaluated the therapeutic effects of iMSC transplantation on brain injury after ischemia-reperfusion using a rat transient middle cerebral artery occlusion model and compared its therapeutic efficacy with that of bone marrow mesenchymal stem cells (BMMSCs). We showed that iMSCs and BMMSCs reduced infarct volumes after reperfusion and significantly improved motor function on days 3, 7, 14, 28, and 56 and cognitive function on days 28 and 56 after reperfusion compared with the vehicle group. Furthermore, immunological analyses revealed that transplantation of iMSCs and BMMSCs inhibited microglial activation and expression of proinflammatory cytokines and suppressed oxidative stress and neuronal cell death in the cerebral cortex at the ischemic border zone. No difference in therapeutic effect was observed between the iMSC and BMMSC groups. Taken together, our results demonstrate that iMSC therapy can be a practical alternative as a cell source for attenuation of brain injury and improvement of neurological function because of the unlimited supply of uniform therapeutic cells.**

## INTRODUCTION

Ischemic stroke causes severe neurological damage and high mortality. Recombinant tissue plasminogen activators and endovascular therapy are clinically effective for treating acute ischemic stroke. However, the eligibility criteria are narrow, and only a limited number of patients can receive recanalization therapy.[1,2] This therapy is reserved for patients in the acute phase, within hours of onset, and aims to recanalize the occluded vessel and rescue the penumbra. Inflammation and oxidative stress following stroke recanalization therapy can result in damage and death of neurons and glial cells, leading to subsequent functional impairment and disability.[3] Conventional neuroprotective therapies targeting these post-infarction pathophysiological responses are limited to use of edaravone as a free radical scavenger in the acute phase, which demonstrates highly limited clinical efficacy.[4,5] In contrast, efficacy of stem cell therapy for acute and chronic cerebral ischemia through multiple channels, which include anti-inflammatory and neuro-angiogenic effects, has been reported in animal models.[6–9] Therefore, stem cell therapy for patients with stroke is attracting attention as a new potential treatment.

The mechanism underlying the therapeutic effect of mesenchymal stem cells (MSCs) on ischemic stroke has been studied extensively.[10–12] MSCs exert their effect through a series of trophic factors that are stimulated by the damaged surrounding environment and directly or indirectly promote repair of ischemic brain tissue. MSCs secrete a variety of neurotrophic factors, including cytokines, chemokines, and extracellular matrix proteins; promote anti-inflammatory and neuroprotective effects; and have angiogenic effects on ischemic brain tissue.[13–17] We have previously demonstrated the therapeutic effect of bone marrow MSCs (BMMSCs) or dental pulp stem cells in transient middle cerebral artery occlusion (tMCAO) model rats.[18,19] In both cases, administration of MSCs to tMCAO model rats resulted in a reduction of infarct volume and improvement of neurological signs. We also demonstrated that the therapeutic effects were mainly mediated by inhibiting neuronal degeneration through suppression of microglial activity and inhibition of inflammatory

Received 21 July 2022; accepted 11 July 2023;
https://doi.org/10.1016/j.omtm.2023.07.005.

[5]These authors contributed equally

**Correspondence:** Yoshitaka Miyagawa, PhD, Department of Biochemistry and Molecular Biology, Nippon Medical School, 1-1-5 Sendagi, Bunkyo-ku, Tokyo 113-8602, Japan.
**E-mail:** yoshitaka-miyagawa@nms.ac.jp
**Correspondence:** Chikako Nito, MD, PhD, Department of Neurological Science, Graduate School of Medicine, Nippon Medical School, 1-1-5 Sendagi, Bunkyo-ku, Tokyo 113-8603, Japan.
**E-mail:** cnito@nms.ac.jp

cytokines, such as tumor necrosis factor alpha (TNF-α) and interleukin-1β (IL-1β). Thus, MSC-based cell therapy holds great promise for treatment of cerebral infarction in the future. In fact, clinical application of BMMSCs is currently being pursued, and clinical trials are underway. In the clinical trial, BMMSCs were administered intracerebroventricularly to patients with subacute ischemic stroke, and the preliminary results showed that intracerebroventricular implantation of autologous BMMSCs was safe and well tolerated.[20] It is anticipated that the demand for MSC-based cell therapy will continue to grow. However, in clinical practice, intracerebroventricular administration of autologous cells to patients is time critical for treatment of acute stroke, and intravenous administration of allogeneic cells is preferable. In addition, several limitations of somatic stem cell-based therapies involving BMMSCs have been identified. First, the procedures for collecting BMMSCs are invasive, and the supply is limited. Second, the properties of BMMSCs vary from donor to donor, making it difficult to obtain uniform cells. Third, the phenotype of MSCs can change during their expansion in a two-dimensional culture.[21] Therefore, there remain many concerns to be solved before clinical use.

Induced pluripotent stem cells (iPSCs) have the inherent properties of unlimited self-renewal and pluripotency. Because of the infinite self-renewal capacity of iPSCs, cells with the same characteristics, or uniformity, can always be produced. In addition, they can be established from the somatic cells of any individual.[22] Hence, iPSCs could be an attractive alternative cell source for cell-based therapy. However, because of the tumorigenic phenotype of iPSCs, it is essential to have a robust and efficient method to generate some necessary cell types without contamination of undesirable cells for safe application of iPSCs for cell therapy.[23] To address these concerns, several methods to differentiate iPSCs into target cells via intermediates have been established, including induction of epicardial cells via lateral plate mesoderm, induction of chondrocytes via limb bud mesenchymal cells, and induction of glomeruli and tubules via nephron progenitor cells.[24–26] For iPSC-derived MSC (iMSC) generation, a differentiation method through the intermediate of neural crest cells (NCCs) has been established.[27] These iMSCs exhibit the general mesenchymal features of BMMSCs; they possess multipotent differentiation potential and express common surface markers of MSCs.[27,28] Furthermore, iMSCs have been reported to have a higher proliferative potential than BMMSCs,[29,30] which suggests that iMSCs may be more readily available than MSCs as a cell source. Currently, iMSCs are being used in dosing studies in various animal disease models, such as lower limb ischemia, inflammatory bowel disease (IBD), and corneal injury, and have been reported to reduce ischemia and exhibit anti-inflammatory effects.[30–32] In stroke models, there have been studies on administration of iMSCs to cerebral hemorrhage model rats and use of iMSC-derived exosomes in rats after ischemic stroke.[33,34] However, the underlying mechanisms of the therapeutic effects have not been fully established, and there have been no comparative studies of the therapeutic effects of iMSCs and BMMSCs following cerebral ischemia-reperfusion injury. Here, we evaluated the efficacy and mechanism of systemic administration of iMSCs in a rat model of focal cerebral ischemia and compared the efficacy of iMSCs with that of BMMSCs.

## RESULTS

### Phenotypic comparison of BMMSCs and iMSCs

To compare the therapeutic efficacy of BMMSCs and iMSCs, human iPSCs (hiPSCs) were differentiated into iMSCs via iPSC-derived NCCs (iNCCs). During induction of iPSCs to iNCCs, the cells grew slowly and showed a morphological change from the typical iPSC shape to a spindle shape (Figure S1A). To enrich iNCC populations from differentiated iPSC cultures, we isolated CD271-positive cells using fluorescence-activated cell sorting (FACS). The morphology of enriched cells was similar to the iNCC morphology, with high expression of CD271, which is a positive marker for NCCs, as described previously (Figures S1B and S1C).[27] The iNCCs were further differentiated into iMSCs by replacing the iNCC medium with an iMSC induction medium. The morphology, expression of surface antigens, and differentiation potential were compared between BMMSCs and iMSCs. The iMSCs showed a fibroblast-like morphology similar to BMMSCs, as described previously (Figure 1A).[35] Immunophenotyping revealed that both MSCs were positive for MSC surface markers (CD73/90/105) (Figure 1B) and negative for surface markers of the hematopoietic lineage (Figure S2). Pluripotent stem cell markers for iPSCs (TRA-1-60, TRA-1-81, and OCT-4) were negative in iMSCs (Figure S3). However, there was a difference in tissue factor CD142 expression, which is a risk factor for thrombus formation in MSC transplantation. A small population of iMSCs showed weak CD142 expression, whereas BMMSCs showed almost no CD142 expression (Figure S4). We investigated the profiles of secreted cytokines from MSCs, and the results are shown in Figure S5. While there were some slight differences in each secreted cytokine, the overall secretion profile was similar between BMMSCs and iMSCs. The differentiation potential of both MSCs into osteoblasts, chondrocytes, and adipocytes was confirmed (Figure 1C). We also performed karyotype analysis for MSCs (Figure S6). Almost all karyotypes were normal in most cases, but instances of non-diploidy were identified in one cell (2%) in BMMSCs and six cells (12%) in iMSCs. These results indicate that iMSCs are almost similar to BMMSCs, with some differences in their properties.

### BMMSC and iMSC administration reduces cerebral infarct volumes in a rat tMCAO model

To assess the therapeutic potential of iMSCs for ischemia-reperfusion (I/R) injury and compare it with that of BMMSCs, BMMSCs and iMSCs were administered intravenously to a rat tMCAO model, and infarct volume was evaluated (Figure 2). The infarct volumes were determined from 2,3,5-triphenyltetrazolium chloride (TTC)-stained sections 3 days after tMCAO (Figure 2A). The results revealed that the mean (±SD) infarct volumes 3 days post tMCAO were significantly lower in the BMMSC ($189.1 \pm 27.7$ mm$^3$, $p = 0.011$) and iMSC ($188.8 \pm 25.3$ mm$^3$, $p = 0.010$) groups than in the vehicle group ($241.9 \pm 16.2$ mm$^3$) (Figure 2B), whereas there was no significant difference between the BMMSC and iMSC groups. The data show that

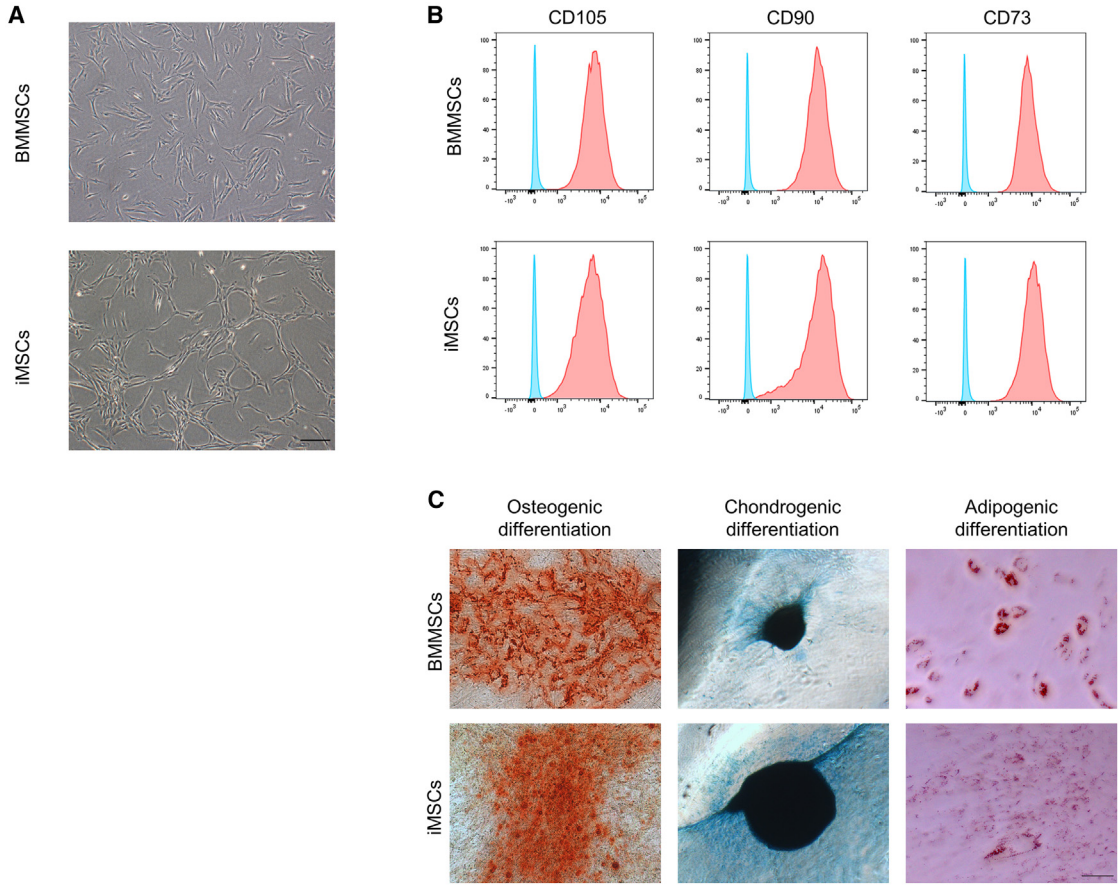


**Figure 1. Characterization of induced mesenchymal stem cells (iMSCs) and bone marrow mesenchymal stem cells (BMMSCs)**

(A) Cell morphology of BMMSCs and iMSCs. Scale bar, 200 μm. (B) Surface marker analyses of iMSCs using flow cytometry. The blue histogram represents the isotype control, and the red overlay represents each antigen. The MSC-positive markers CD90, CD73, and CD105 were measured. (C) Comparison of the differentiation potential between BMMSCs and iMSCs. MSCs were differentiated into osteogenic (left), chondrogenic (center), and adipogenic (right) lineages and stained by alizarin red for osteocytes, Alcian blue for chondrocytes, and oil red O for adipocytes. Scale bar, 200 μm.

BMMSCs and iMSCs can reduce infarct volume in the tMCAO model.

### BMMSC and iMSC delivery improves neurological outcomes

We next examined whether iMSC transplantation could improve neurological outcomes after I/R injury (Figure 3). Neurological scores and motor function were investigated 3, 7, 14, 28, and 56 days after tMCAO. On all days analyzed, the BMMSC and iMSC groups showed significant improvements in posture score (Figure 3A; BMMSCs 3 days, $p = 0.021$; BMMSCs 7 days, $p = 0.003$; BMMSCs 14 days, $p = 0.029$; BMMSCs 28 days, $p = 0.003$; BMMSCs 56 days, $p = 0.017$; iMSCs 3 days, $p = 0.013$; iMSCs 7 days, $p = 0.005$; iMSCs 14 days, $p = 0.005$; iMSCs 28 days, $p = 0.013$; iMSCs 56 days, $p = 0.003$) and palsy score (Figure 3B; BMMSCs 3 days, $p = 0.003$; BMMSCs 7 days, $p = 0.017$; BMMSCs 14 days, $p = 0.006$; BMMSCs 28 days, $p = 0.002$; BMMSCs 56 days, $p = 0.017$; iMSCs 3 days, $p = 0.003$; iMSCs 7 days, $p = 0.001$; iMSCs 14 days, $p = 0.006$; iMSCs 28 days, $p = 0.002$; iMSCs 56 days, $p = 0.001$) compared with the vehicle group. Motor function was also ameliorated in the BMMSC and iMSC groups compared with the vehicle group, as assessed using rotarod performance (Figure 3C; BMMSCs 3 days, $p = 0.031$; BMMSCs 7 days, $p = 0.035$; BMMSCs 14 days, $p = 0.016$; BMMSCs 28 days, $p = 0.01$; BMMSCs 56 days, $p = 0.032$; iMSCs 3 days, $p = 0.033$; iMSCs 7 days, $p = 0.017$; iMSCs 14 days, $p = 0.049$; iMSCs 28 days, $p = 0.007$; iMSCs 56 days, $p = 0.029$) and forelimb grip strength (Figure 3D; BMMSCs 3 days, $p = 0.005$; BMMSCs 7 days, $p = 0.005$; BMMSCs 14 days, $p = 0.006$; BMMSCs 28 days, p 0.024; BMMSCs 56 days, $p < 0.001$; iMSCs 3 days, $p = 0.002$; iMSCs 7 days, $p < 0.001$; iMSCs 14 days, $p < 0.001$; iMSCs 28 days, $p = 0.002$; iMSCs 56 days, $p < 0.001$), whereas no significant difference in neurological improvement was observed between the BMMSC and iMSC groups. To assess the effect of MSC administration on spatial memory, we also examined cognitive function 30 and 56 days after tMCAO using the Y-maze test (Figure 3E). On both days post administration of MSCs, there was a significant improvement in spatial memory in the BMMSC and iMSC groups compared

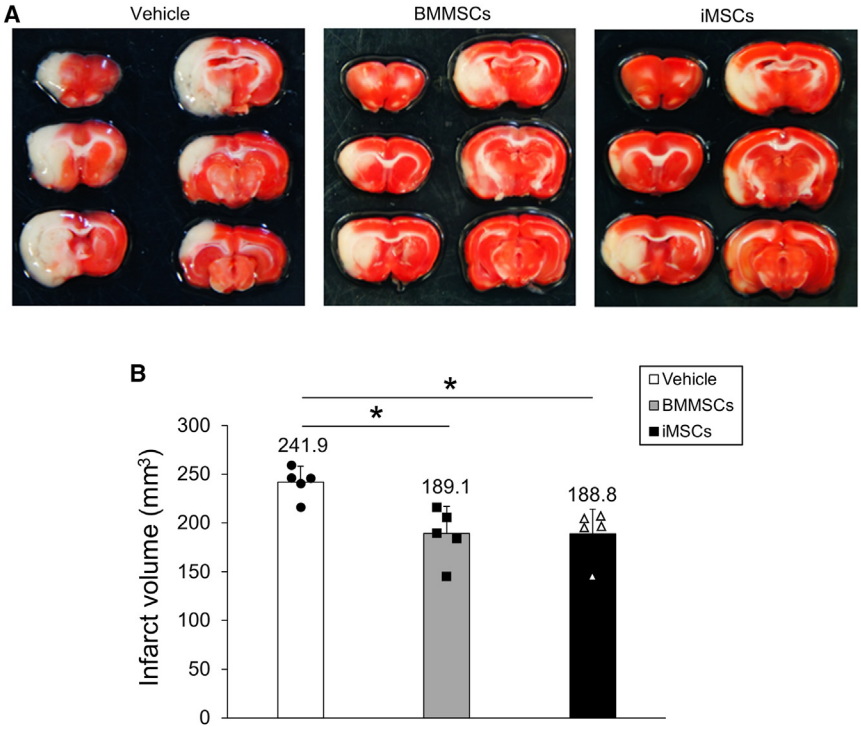


**Figure 2. Reduction of infarct volume by administration of BMMSCs and iMSCs**

(A) 2,3,5-Triphenyl tetrazolium chloride (TTC) staining of rat brains in the vehicle-treated (left), BMMSC-treated (center), and iMSC-treated (right) groups. Sprague-Dawley rats were subjected to transient middle cerebral artery occlusion (tMCAO) and then injected intravenously with BMMSCs, iMSCs, or PBS. The infarct volumes were analyzed by TTC staining 3 days after tMCAO. In TTC staining, normal tissue is stained red, and the infarcted area is unstained. Six sections from one rat brain divided into sections of 2 mm each are shown. One representative rat brain per vehicle, BMMSC, and iMSC group is displayed. (B) Quantitative analysis of the infarct volumes 3 days post tMCAO in each group. The data presented are the means and SDs (*$p < 0.05$, $n = 5$ for each group).

with the vehicle group (BMMSCs 28 days, 0.785 ± 0.125, $p = 0.002$; iMSCs 28 days, 0.784 ± 0.076, $p = 0.002$; vehicle 28 days, 0.581 ± 0.101; BMMSCs 56 days, 0.762 ± 0.133, $p = 0.017$; iMSCs 56 days, 0.740 ± 0.126, $p = 0.038$; vehicle 56 days, 0.581 ± 0.093), whereas there was no significant difference between the spatial memory of the BMMSC and iMSC groups. Together, our results suggest that administration of iMSCs significantly improved neurological and motor function in the short and long term and cognitive function in the long term, showing effects similar to BMMSCs.

### BMMSC and iMSC administration suppresses microglial activation and proinflammatory cytokine levels

To explore the mechanism by which transplantation of iMSCs improves neurological outcomes after I/R injury, we examined the activity of microglia in the cerebral cortex at the ischemic border zone (IBZ) as an evaluation of the anti-inflammatory effect of iMSCs (Figure 4A). Ionized calcium-binding adaptor molecule 1 (Iba-1) is a microglial marker, and its expression is associated with microglia activated by ischemic brain injury. Therefore, we analyzed the localization of Iba-1 in the cortical IBZ to assess microglial activation after MSC transplantation (Figure 4B). We observed that the numbers of Iba-1-positive cells in the BMMSC and iMSC groups were significantly lower than those in the vehicle group 3 days post tMCAO (BMMSCs, $p < 0.001$; iMSCs, $p < 0.001$) (Figure 4C), whereas the number of Iba-1-positive cells in the iMSC group was comparable with that in the BMMSC group, demonstrating that iMSCs exerted a significant inhibitory effect on microglial activation in the penumbra region of the ischemic side of the brain cortex, comparable with that of BMMSCs.

To further explore the anti-inflammatory effects of iMSCs in the tMCAO model, proinflammatory cytokine levels were assessed in the whole ischemic side of the brain and cortical IBZ (Figure 4D). To this end, we evaluated the distribution of TNF-α in the ischemic brain and the levels of IL-1β and IL-6 in the ischemic side of the brain. On day 3 post tMCAO, the BMMSC and iMSC groups showed a significant reduction in the number of TNF-α-positive cells compared with the vehicle group (BMMSCs, $p = 0.018$; iMSCs, $p = 0.013$) (Figure 4E). There was no significant difference in the number of TNF-α-positive cells in the BMMSC and iMSC groups. Furthermore, IL-1β (BMMSCs, $p = 0.046$; iMSCs 3 days, $p = 0.024$) and IL-6 levels (BMMSCs, $p = 0.048$; iMSCs, $p = 0.027$) in the brain in the BMMSC and iMSC groups were significantly lower than in the vehicle group (Figures 4F and 4G), whereas no notable differences were observed in terms of IL-1β and IL-6 levels between the BMMSC and iMSC groups. We also identified TNF-α-expressing cells in the cerebral cortex of the IBZ using fluorescent staining. Neurons were identified with neuronal nuclei (NeuN), microglia with OX42, blood vessels with RECA-1, and astrocytes with glial fibrillary acidic protein (GFAP), plus multiple staining for TNF-α for each specimen in the brain sections (Figure S7A). TNF-α was significantly expressed in NeuN- and OX42-positive cells compared with RECA-1- and GFAP-positive cells (NeuN, $p < 0.001$; OX42, $p < 0.001$; Figure S7B). There was no significant difference in TNF-α expression between NeuN- and OX42-positive cells. The number of NeuN/TNF-α-positive cells was significantly lower in the BMMSC group ($p = 0.027$) and tended to be lower in the iMSC group compared with the vehicle group (Figures 5A and 5B), whereas there was no significant difference between the BMMSC and iMSC groups. The number of OX-42/TNF-α-positive cells was not significantly different between the vehicle, BMMSC, and iMSC groups (Figures S8A and S8B). Overall, these observations indicate that iMSC administration results in a significant reduction in proinflammatory cytokine expression in the tMCAO model.

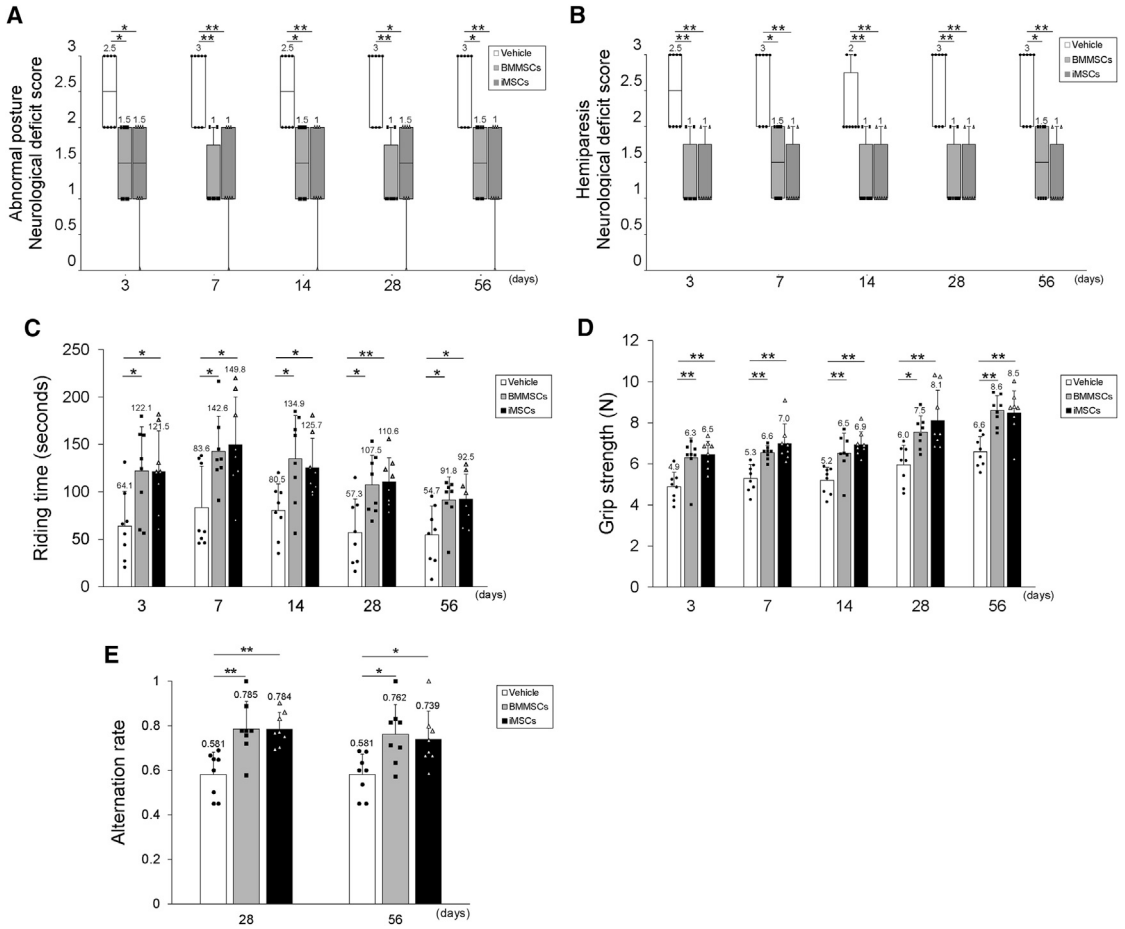


**Figure 3. Improvement of neurological score, motor function, and cognitive function by administration of BMMSCs and iMSCs**

(A and B) Abnormal posture (A) and hemiparesis (B) assessment 3, 7, 14, 28, and 56 days after tMCAO in vehicle-, BMMSC-, and iMSC-transplanted reperfusion groups. Boxplots indicate the median and IQR, and whiskers indicate the maximum and minimum values (*$p < 0.05$, **$p < 0.01$; n = 8 for each group). (C and D) Rotarod performance (C) and forelimb grip strength (D) assessment 3, 7, 14, 28, and 56 days after tMCAO in vehicle-, BMMSC-, and iMSC-transplanted reperfusion groups. Data are presented as mean ± SD (*$p < 0.05$, **$p < 0.01$; n = 8 for each group). (E) Improvement of spatial working memory 28 and 56 days after tMCAO. Shown is the alternation rate in the Y-maze spontaneous test in the vehicle-, BMMSC-, and iMSC-treated groups. Data are presented as mean ± SD (*$p < 0.05$, **$p < 0.01$; n = 8 for each group).

### BMMSC and iMSC administration inhibits oxidative stress

Given that iMSC administration yielded anti-inflammatory effects in the tMCAO model, we hypothesized that iMSCs might also reduce oxidative stress in the whole ischemic brain and the cortical IBZ. Hence, we examined the distribution of 4-hydroxynonenal (4-HNE) and 8-hydroxy-20-deoxyguanosine (8-OHdG), which are markers of lipid peroxidation and oxidative DNA damage, respectively, in the ischemic brain and the activity of superoxide dismutase (SOD), a type of antioxidant enzyme, throughout the ischemic side of the brain. We assessed the localization of 4-HNE-positive cells in the cortical IBZ using immunohistochemical staining (Figure 6A), which revealed that the number of 4-HNE-positive cells (BMMSCs, $p = 0.005$; iMSCs, $p < 0.001$; Figure 6B) was significantly reduced in the BMMSC and iMSC groups compared with the vehicle group 3 days post tMCAO. Similarly, the localization of 8-OHdG-positive cells in the cortical IBZ on day 3 post tMCAO was examined (Figure 6C) and was significantly lower in both cell-treated groups than in the vehicle group (BMMSCs, $p = 0.003$; iMSCs, $p = 0.002$; Figure 6D). Consistent with the reduction in 4-HNE and 8-OHdG distribution, the overall SOD activity was significantly higher in the BMMSC and iMSC groups compared with the vehicle group (BMMSCs, $p = 0.012$; iMSCs, $p = 0.030$; Figure 6E). No major differences in 4-HNE and 8-OHdG distribution and SOD activity were observed between the BMMSC and iMSC groups. Collectively, these results demonstrate the suppressive effect of BMMSCs and iMSCs on I/R injury-induced oxidative stress in the rat brain.

### BMMSC and iMSC administration inhibits ischemia-induced neuronal damage

We further confirmed the inhibition of apoptosis and neuroprotective effect of iMSCs in the tMCAO model by performing terminal

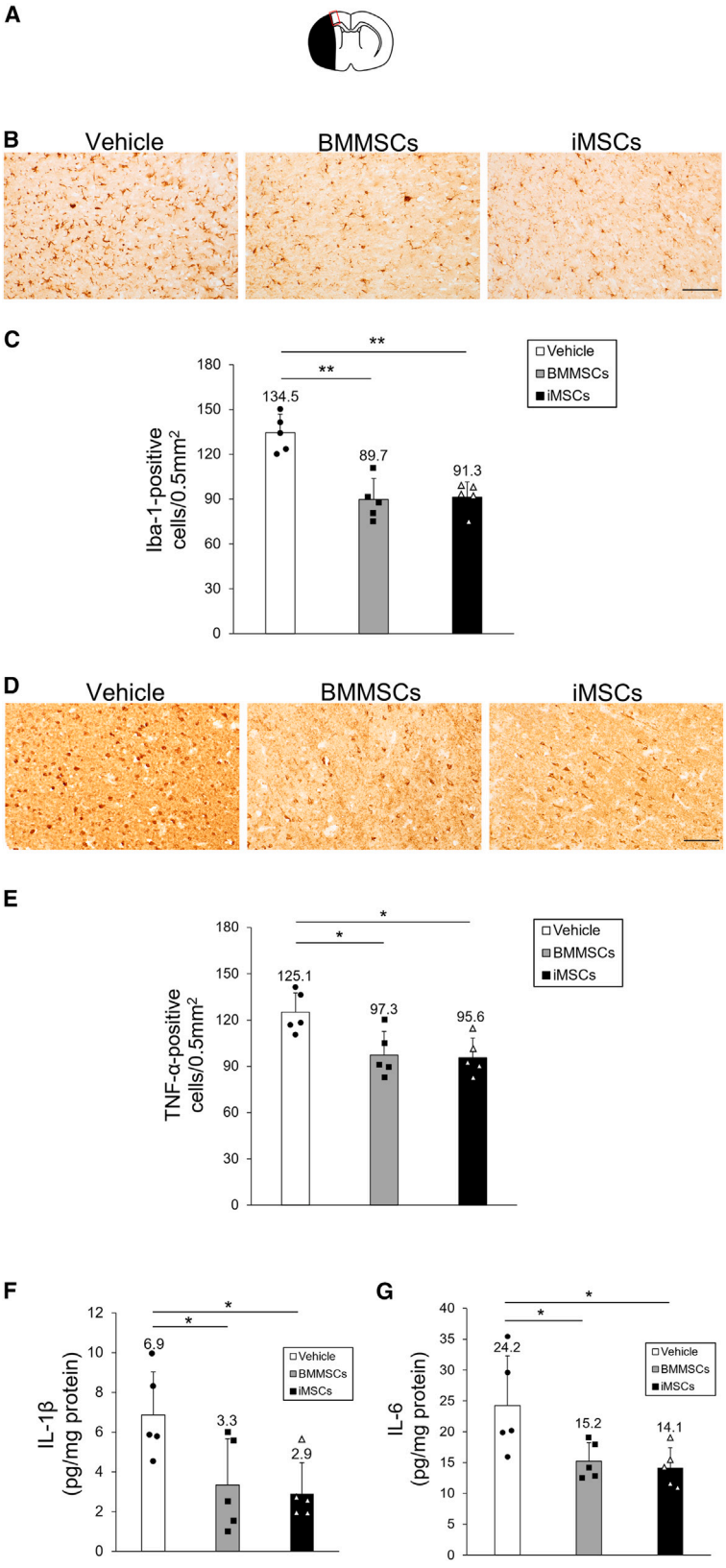


**Figure 4. Evaluation of microglial activity and proinflammatory cytokine levels in the ischemic side of the brain**

(A) Schematic of the cortical IBZ. The red-lined square on the brain map shows the cortical IBZ. The black area represents the ischemic lesion. (B) Iba-1 staining in rat brain sections treated with vehicle (left), BMMSCs (center), and iMSCs (right). Scale bar, 100 μm. (C) Quantification of Iba-1-positive cells in the rat brain with or without MSC treatment. Data are presented as mean ± SD (**$p < 0.01$, $n = 5$ for each group). (D) TNF-α staining in rat brain sections treated with vehicle (left), BMMSCs (center), and iMSCs (right). Scale bar, 100 μm. (E) Quantification of TNF-α-positive cells in the rat brain with or without MSC treatment. Data are presented as mean ± SD (*$p < 0.05$; $n = 5$ for each group). (F and G) Quantification of IL-1β (F) and IL-6 (G) expression in ischemic hemisphere extracts. Data are presented as mean ± SD (*$p < 0.05$, $n = 5$ for each group). Sprague-Dawley rats were treated with tMCAO and injected intravenously with BMMSCs, iMSCs, or PBS. Three days after tMCAO, brain sections were stained with anti-Iba-1 or anti-TNF-α antibodies. The ischemic hemisphere extracts were also analyzed using ELISA.

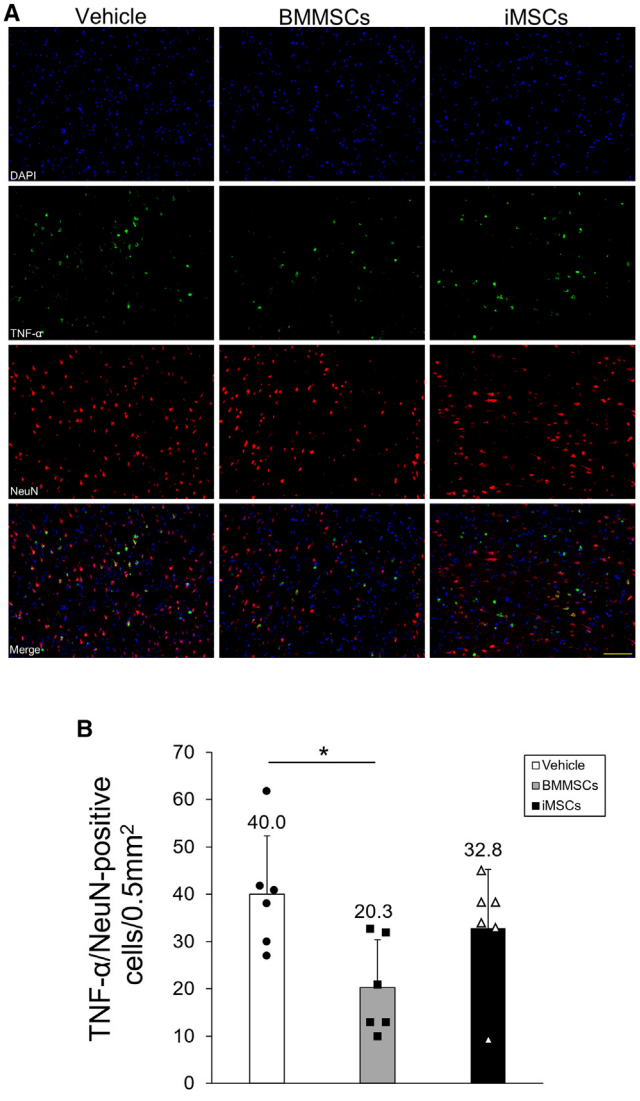


**Figure 5. Localization of TNF-α expression in the ischemic side of the brain**

(A) Localization of TNF-α (green) and NeuN (red) expression in rat brain sections treated with vehicle (left vertical column), BMMSCs (center vertical column), and iMSCs (right vertical column). Scale bar, 100 μm. Nuclei were stained in blue with DAPI. Merge overlays of three fluorescence images are shown in the bottom row. (B) Quantification of TNF-α-positive neurons in the rat brain. Data are shown as mean ± SD (*$p < 0.05$, n = 6 for each group).

deoxynucleotidyl transferase (TdT)-mediated deoxyuridine triphosphate (dUTP) nick end labeling (TUNEL) staining and Fluoro-Jade C (FJC) staining in the cortical IBZ 3 days post tMCAO. Analysis of TUNEL-positive cells in the cortical IBZ (Figure 7A) showed that the number of TUNEL-positive cells was significantly lower in the iMSC group than in the vehicle group ($p = 0.038$). The number of TUNEL-positive cells was also lower in the BMMSC group than in the vehicle group (Figure 7B). We also analyzed FJC-positive cells in the cortical IBZ (Figure 7C) and found that treatment with BMMSCs and iMSCs similarly decreased the number of FJC-positive cells compared with the vehicle group (BMMSCs, $p = 0.027$; iMSCs, $p = 0.038$) (Figure 7D). These results support the neuroprotective effect of BMMSCs and iMSCs in the rat brain.

### Biodistribution and quantification of engrafted MSCs

The biodistribution and quantification of transplanted MSCs at 72 h using real-time PCR with human-specific Alu sequences are shown in Figure 8. In both cases, a considerably small amount of human DNA was detected in the investigated tissues. BMMSCs and iMSCs were mainly distributed in the liver; however, iMSCs were detected more in the liver than BMMSCs ($p < 0.001$). MSCs were also detected in other organs, such as the lungs for BMMSCs and the femur for iMSCs, although in smaller amounts than in the liver. This result indicates that iMSCs remained predominantly distributed in the liver more than BMMSCs.

## DISCUSSION

In the present study, we compared the therapeutic potential of iMSCs in focal cerebral ischemic rats with that of BMMSCs and found that iMSCs significantly reduced infarct volumes and enhanced motor and cognitive function recovery, similar to BMMSCs. We also demonstrated the anti-inflammatory effects of iMSCs via suppression of microglial activity and decreased expression of anti-inflammatory cytokines (TNF-α, IL-1β, and IL-6) and antioxidant stress effects, based on the decreased expression of 4-HNE and 8-OHdG and increased SOD activity in a rat cerebral ischemic model. Together, our results showed that iMSCs can be a new therapeutic source to replace BMMSCs for cellular therapy of cerebral infarction.

Stem cell therapy using human MSCs (hMSCs) is being considered as a new treatment for cerebral infarction because of the time constraints of conventional therapy and the limited number of patients who can be treated. hMSCs, especially BMMSCs, have previously shown efficacy and safety *in vivo* in a rat model of cerebral infarction,[36–41] and clinical trials are currently underway worldwide.[1,42–44] However, BMMSCs are problematic because they require invasive techniques for isolation, and expansion of sufficient numbers of BMMSCs for cell therapy remains a challenge. Moreover, the quality of BMMSCs is affected by the age and health of the donor, making it difficult to obtain cells with uniform characteristics.[45–47] MSCs also deteriorate rapidly during the expansion process in *in vitro* culture[48–50]; thus, their therapeutic effects are not always stable. iMSCs generated from iPSCs, which are cells with unlimited self-renewal capacity and pluripotency, have the potential to improve upon BMMSCs in terms of uniformity of properties and proliferative capacity. Hence, it is worth considering the potential of iMSCs as a new source of cells to replace BMMSCs in cell therapy for cerebral infarction.

MSCs, including BMMSCs, are defined by the following three basic criteria proposed by the International Society for Cell Therapy.[51] First, they adhere to plastic when maintained under standard culture conditions. Second, they express the surface antigen markers CD105, CD73, and CD90 and are negative for CD45, CD34, CD14 or CD11b, CD79α, or CD19 and human leukocyte antigens-DR (HLA-DR).

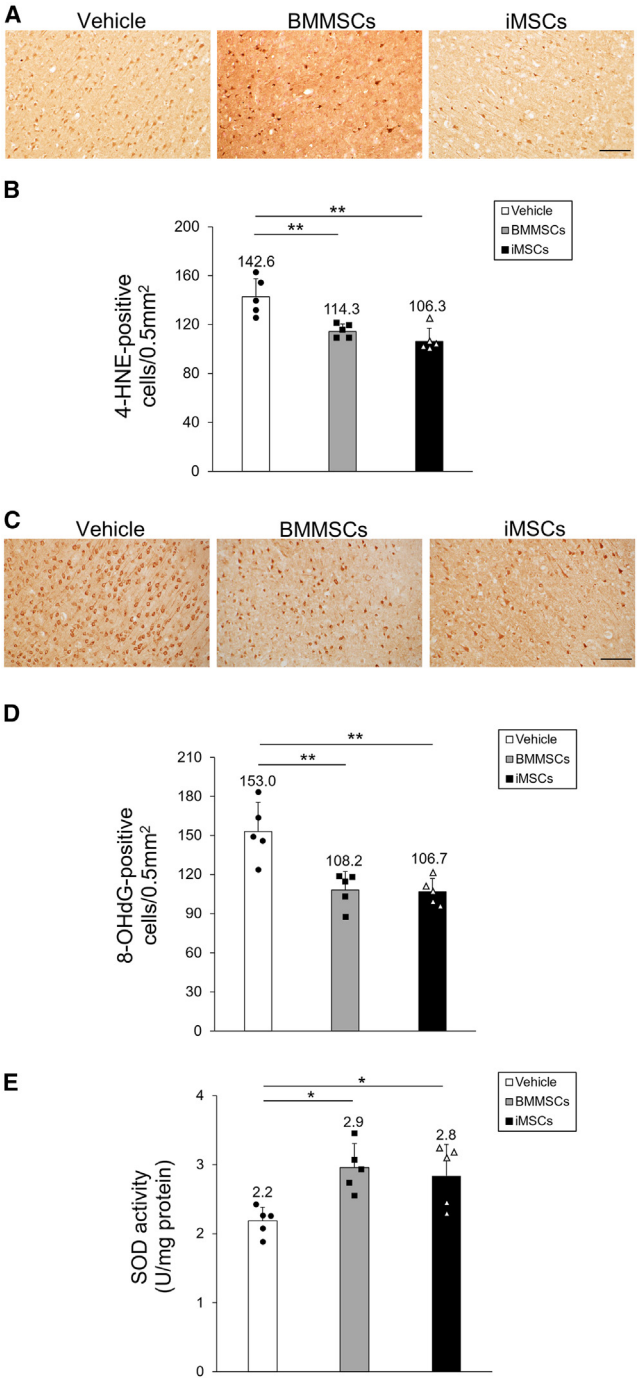


**Figure 6. Evaluation of oxidative stress in the ischemic side of the brain**

(A and C) 4-Hydroxynonenal (4-HNE) (A) and 8-hydroxy-20-deoxyguanosine (8-OHdG) (C) staining in rat brain sections treated with vehicle (left), BMMSCs (center), and iMSCs (right). Scale bar, 100 μm. (B and D) Quantification of 4-HNE-positive (B) and 8-OHdG-positive (D) cells in the rat brain with or without MSC treatment. Data are presented as mean ± SD (**$p < 0.01$, $n = 5$ for each group). (E) Total SOD activity in ischemic hemisphere extracts. Data are presented as mean ± SD (*$p < 0.05$, $n = 5$ for each group). SD rats were treated with tMCAO and injected intravenously with BMMSCs, iMSCs, or PBS. Three days after tMCAO, brain sections were stained with anti-4-HNE or anti-8-OHdG antibodies. The ischemic hemisphere extracts were also analyzed using a SOD assay kit.

Third, MSCs exhibit differentiation potential for three lineages *in vitro*: osteoblasts, adipocytes, and chondroblasts. In the present study, we demonstrated that iMSCs, through iNCC intermediates, showed a similar surface profiles and adipogenic, osteogenic, and chondrogenic differentiation potential (Figures 1 and S1). In addition, previous studies have reported that unique markers of pluripotent stem cells in iPSCs, such as Oct-4, TRA1-60, and TRA-1-81, are negative in iMSCs,[52,53] which was partly consistent with the results of the present study. Thus, iMSCs used in this study fulfill the critical criteria. Notably, there are a few differences in secreted cytokines between iMSCs and BMMSCs, such as the inflammation-related IL-1, stress-responsive mitogen-activated protein kinase 1/2 signaling,[54] expression levels of certain surface markers,[55,56] and differentiation potential.[52,57] It will be of interest to determine whether these differences affect the neuroprotective and therapeutic effects of iMSCs. In contrast, several studies have also developed induction methods for iMSCs derived from iPSCs and compared iMSCs with BMMSCs *in vitro*[53,58–60]; iMSCs are similar to BMMSCs in morphology and MSC-specific gene expression, regardless of differences in induction methods.[55,61–63] In this study, we enriched iMSCs by flow cytometry sorting to eliminate the potential risk of tumor formation by undifferentiated iPSCs in the process of iMSC induction. Moreover, although several iMSC induction methods without cell sorting have been developed,[64,65] iMSCs generated by these methods showed varied MSC marker expression[64,65] and might include residual undifferentiated iPSCs. It remains to be elucidated whether induction and culture methods affect the properties and cell therapeutic effect of iMSCs against inflammatory diseases. A previous study has demonstrated that repeated passaging of iMSCs resulted in decreased expression levels of MSC markers,[27] which is consistent with our preliminary results. Therefore, further investigation is required to determine the effect of passage number on the properties and therapeutic efficacy of iMSCs. While we established that iMSCs cause a reduction of cerebral infarct volume and exhibit anti-inflammatory effects, iMSCs generated using our method included a few non-diploid cells (Figure S6). However, karyotypic abnormalities in cell therapy can pose a safety risk and affect the therapeutic efficacy of cell therapy.[66] Therefore, future efforts to improve genomic instabilities could further expand the therapeutic potential of iMSC-based cell therapy.

Because of the advantages of iMSC use for cell therapy, we and other groups have hypothesized that iMSCs could be harnessed as an alternative source of hMSCs to overcome the existing concerns with MSC-based therapy for brain injury. Chen et al.[33] have reported the effect of iMSC administration in a rat model of cerebral hemorrhage. They reported that iMSCs can reduce the volume of cerebral infarction after cerebral hemorrhage through anti-inflammatory effects and antioxidant stress, although no comparative studies with hMSCs have been conducted. To the best of our knowledge, our study is the first report clearly comparing the therapeutic effects of iMSCs and

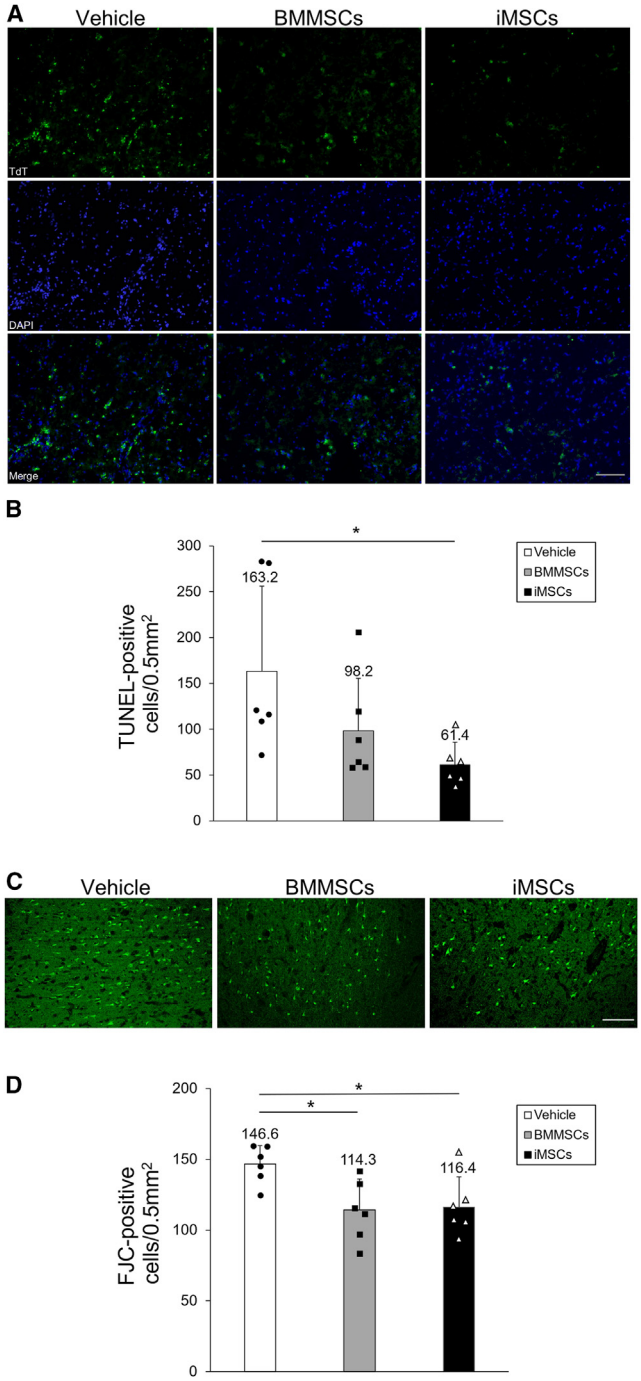


**Figure 7. Evaluation of apoptosis and neuronal degeneration in the cortical ischemic boundary zone**

(A) Apoptosis was detected by TdT-mediated dUTP nick end labeling (TUNEL) staining (top panels) in the vehicle (left vertical column), BMMSC (center vertical column), and iMSC groups (right vertical column). Nuclei were stained in blue with DAPI (center panels). Merge overlays of two fluorescence images are shown in the bottom panels. (B) Quantification of TUNEL-positive neurons in the rat brain. Data are shown as mean ± SD (*$p < 0.05$, n = 6 for each group). (C) Fluoro-Jade C (FJC) staining in rat brain sections treated with vehicle (left), BMMSCs (center), and iMSCs (right). Scale bar, 100 μm. (D) Quantification of FJC-positive cells in the rat brain with or without MSC treatment. Data are presented as mean ± SD (*$p < 0.05$, n = 6 for each group). Sprague-Dawley rats were treated with tMCAO and injected intravenously with BMMSCs, iMSCs, or PBS. FJC staining was performed 3 days after tMCAO.

BMMSCs in a rat cerebral ischemic model and revealing that the therapeutic effects were comparable between iMSCs and BMMSCs. Our findings contribute to accelerating the clinical application of iMSCs for treatment of cerebrovascular diseases. In addition, the therapeutic effects of iMSCs have been confirmed not only using cerebral ischemia models but also various other disease models.[30,31,67] In the mouse IBD model, administration of iMSCs has been shown to improve intestinal inflammation by increasing the number of regulatory T cells and decreasing infiltration of macrophages and neutrophils into the colonic submucosa, with the therapeutic effects of iMSCs demonstrated to be mediated via anti-inflammatory and anti-apoptotic effects.[31] In mouse models of chemical and mechanical damage to the cornea, iMSC treatment markedly reduced the inflammatory infiltrate of the cornea and decreased the levels of TNF-α, IL-1β, and IL-6 in the cornea.[32] Thus, iMSCs have been reported to exhibit anti-inflammatory effects not only in cerebral infarction but also in a variety of other inflammatory diseases, and the scope of clinical application of iMSCs is expected to expand further in the future.

It was previously thought that the administered MSCs migrate directly to and are mainly biodistributed in damaged organs; however, it has been confirmed that the rate of differentiation into damaged organs is extremely low.[68] In the present study, we evaluated the biodistribution of BMMSCs and iMSCs on the third day after administration and confirmed that they were mainly distributed in the organs of the body, such as the liver. Although many previous reports have examined biodistribution 24 h after administration, the tendency to distribute to internal organs rather than the brain remains the same.[69,70] These findings suggest that the therapeutic effect of MSC administration in cerebral infarction is not primarily due to their biogenesis and differentiation in the damaged brain. Previous studies have shown that mechanisms related to the therapeutic effects of intravenous administration of BMMSCs in the acute phase of stroke may be due to direct secretion of paracrine factors by stem cells; accumulation of stem cells in the spleen; paracrine effects of various trophic and fluidity factors, such as growth factors and cytokines, via the spleen; and subsequent suppression of inflammatory cytokines.[71–74] Furthermore, a number of mechanisms have been proposed to support a role of BMMSCs administered for neurological diseases, including stroke. SDF-1 is a member of the chemokine subfamily that acts protectively against apoptosis and promotes cell mobilization.[75,76] BMMSCs express SDF-1 and exert neuroprotective effects.[77,78] They also act in various disease modifications with diverse functions, such as promoting remyelination via janus kinase (JAK)/STAT3,[79] intra-neural angiogenesis via vascular endothelial growth factor A, nerve regeneration, and neurotrophic potential.[80,81] Treatment of rats with BMMSCs resulted in decreased expression and secretion of proinflammatory cytokines, such as TNF-α, IL-1β, and

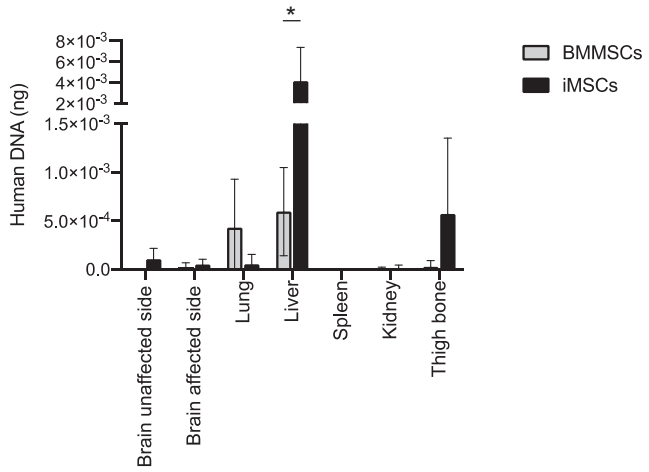


**Figure 8. Biodistribution and quantification of engrafted MSCs**

Shown are biodistribution and quantification of viable BMMSCs (n = 7) and iMSCs (n = 8) 72 h after tMCAO using Alu-based real-time PCR. Values represent the amount of human DNA in 100 ng of total DNA per organ sample. Data are presented as mean ± SD (*$p < 0.01$).

IL-6, in the ischemic side of the brain as well as decreased microglial activity.[18,82] We investigated the diverse profile of iMSC-secreted factors, including SDF-1, and found trends similar to the secretion profile of BMMSCs. Additionally, our study revealed that iMSCs also suppressed inflammatory cytokines, such as TNF-α, and microglial activity in the cortical IBZ and inhibited secretion of inflammatory cytokines, such as IL-1β and IL-6, in the ischemic side of the brain. Therefore, iMSCs have, at least in part, a therapeutic effect on neurological disorders via neuroprotective cytokine secretion.

In addition, expression of 4-HNE and 8-OHdG in the cortical IBZ was decreased in the present study, and activity of SOD, an antioxidant enzyme, was higher in the cell-treated group than in the vehicle group in the ischemic side of the brain, indicating that iMSCs have antioxidant stress effects in the same manner as BMMSCs. In a rat model of cerebral infarction, administration of BMMSCs reduced superoxide and lipid peroxide by-products in the ischemic brain,[83] suggesting that MSCs inhibit cerebral I/R injury through their antioxidant stress effects. Similar anti-inflammatory and antioxidant stress effects of iMSCs were observed in a rat model of cerebral hemorrhage.[33] These observations confirm that iMSCs have neuroprotective effects on the brain through anti-inflammatory and anti-oxidative stress effects via the same mechanism as that of hMSCs. Such inflammatory and antioxidant stress effects can be further enhanced by gene transfer into MSCs. We have demonstrated previously that introduction of IL-10 and hepatocyte growth factor into hMSCs can extend their anti-inflammatory effects.[18,19] Therefore, it may be possible to further increase the therapeutic effect of iMSCs derived from genetically engineered iPSCs.

We successfully demonstrated that administration of iMSCs reduced cerebral infarct volume after tMCAO and significantly improved motor and cognitive functions and that the therapeutic effects of iMSCs were equivalent to those of BMMSCs. Although the neuroprotective effects on the rat brain by iMSCs have been investigated, to the best of our knowledge, only short-term effects have been shown.[33] Our study clearly showed that iMSCs and BMMSCs similarly improved motor and cognitive functions after cerebral infarction, and the therapeutic effects were sustained over the long term, up to at least 56 days (Figure 3). Previous studies have also shown long-term therapeutic effects of BMMSCs in rat and mouse tMCAO models.[84–86] Administration of hBMMSCs to the tMCAO model improves motor and cognitive function from the early phase of administration to 28 days afterward and promotes neurogenesis associated with angiogenesis in the late stages of stroke[85] and proliferation of intrinsic endogenous neural stem cells and neural maturation of neuroblasts in the subventricular zone of the hippocampus.[84] Although promotion of angiogenesis and neurogenesis may contribute to the long-term improvement of neurological function after cerebral infarction, the underlying mechanism remains unclear. Recent studies suggest that extracellular vesicles secreted from BMMSCs and iMSCs promote angiogenesis in a rodent tMCAO model[34,87,88] and can function in iMSCs to improve long-term prognosis through a mechanism similar to that of hBMMSCs. However, further investigation is required to explore the therapeutic mechanism.

We found that the therapeutic effects of iMSCs were equivalent to those of BMMSCs in the tMCAO model in this study. BMMSCs have limitations in expansion culture because the cells deteriorate *in vitro,* as discussed above. Another report has compared the immunomodulatory potential of iMSCs and BMMSCs via natural killer (NK) cells *in vitro*.[89] iMSCs and BMMSCs were co-cultured with IL-2-activated NK cells to examine their immunomodulatory potential, and iMSCs were found to be more effective than BMMSCs. Similarly, iMSCs decreased the cytotoxicity of NK cells by decreasing the expression of inflammatory markers and inhibiting the secretion of cytotoxic granules. Notably, iMSCs maintain immunomodulatory activity at a higher number of passages compared with BMMSCs, suggesting that iMSCs could be superior over long-term passage.

Recently, it has been reported that the risk of thromboembolism from infusion of MSC products expressing hypercoagulable tissue factor (TF/CD142) should be examined[90] and that the expression level of TF/CD142 varies in MSCs derived from different human sources. BMMSCs have the lowest TF/CD142 expression, perinatal tissue-derived MSCs show intermediate expression, and adipose tissue-derived MSCs display the highest expression.[91] Thus, to use MSC products safely, it has been advocated to evaluate whether TF/CD142 is expressed. However, the risk of thromboembolism from MSC products can be reduced by use of appropriate anticoagulants and removal of TF/CD142-positive cells.[89] iMSCs generated in this study contained a small number of CD142-positive cells. Therefore, although future studies should determine whether CD142 is the sole determinant of thromboembolism risk, use of anticoagulants or removal of CD142-positive cells should be considered for safe

clinical application of iMSCs. Ongoing efforts in one of our labs aim to generate CD142-negative iMSCs by alternative differentiation strategies.

In addition, although serum-containing medium was used for MSC preparation in this study, it is necessary to use xeno-free medium for clinical application of MSCs. Recently, xeno-free media have been developed for MSC culture, and characterization of MSCs has also been conducted, showing that the phenotype, differentiation ability, and immunomodulatory capacity of MSCs are maintained.[92] Moreover, MSCs cultured in a serum-free medium showed more significant anti-inflammatory effects than MSCs cultured in a serum medium.[93] While we suspect that iMSCs can be expanded using xeno-free medium without losing their neuroprotective effects, this remains to be demonstrated.

In conclusion, iMSC transplantation in the acute phase of ischemic stroke provides neuroprotective effects via anti-inflammatory and antioxidant stress effects equivalent to BMMSCs. Hence, iMSCs could be an attractive alternative to BMMSCs as a source of cells for cell transplantation for treatment of stroke.

## MATERIALS AND METHODS

### Ethics statement

The experimental protocols dealing with human or animal subjects were approved by the Ethics Committee of the Department of Medicine and Graduate of Nippon Medical School.

### Cells

The hiPSC cell line Nips B2 (HPS0223)[94] was purchased from the Institute of Physical and Chemical Research (RIKEN) Bio Research Resource Center through the National Bio-Resource Project of the Ministry of Education, Culture, Sports, Science and Technology (MEXT)/ Japan Agency for Medical Research and Development (AMED), Japan. hiPSCs were cultured in essential 8 medium (Thermo Fisher Scientific, Waltham, MA, USA) in six-well plates coated with Matrigel (Corning, Corning, NY, USA). The BMMSCs were provided by Kaneka (Tokyo, Japan), and the manufacturing process of BMMSCs was as follows. Human bone marrow was purchased from AllCells (Emeryville, CA, USA); 50 mL of bone marrow was diluted 4-fold with minimum essential medium α (MEM α) (Life Technologies, Carlsbad, CA, USA) supplemented with 10% fetal bovine serum (FBS; Cytiva, Tokyo, Japan) and 1% antibiotic-antimycotic (Thermo Fisher Scientific). The culture-containing bone marrow solution was cultured using CellStack (Corning). The culture medium was changed every 3–4 days, and BMMSCs were collected and cryopreserved after 2 weeks of incubation. BMMSCs were cultured in MSCGM (Lonza, Basel, Switzerland) at 37°C in 98% humidity and 5% $CO_2$.

### Induction of iNCCs from iPSCs

The differentiation method for hiPSC-derived iMSCs was applied as described previously.[27] Briefly, as pre-induction, hiPSCs were cultured in an mTESR1 medium (STEMCELL Technologies, Vancouver, BC, Canada) in cell culture plates coated with growth factor-reduced Matrigel (Corning) for a few days. Post preincubation, hiPSCs were differentiated into iNCCs by replacing the mTESR1 medium with a chemically defined medium (CDM)[95] supplemented with 10 μM SB431542 (Sigma-Aldrich, St. Louis, MO, USA) and 1 μM CHIR99021 (Fujifilm Wako, Osaka, Japan). CDM contained Iscove's modified Dulbecco's medium/Ham's F-12 1:1, 1× chemically defined lipid concentrate (Gibco, Grand Island, NY, USA), 15 μg/mL apo-transferrin (Sigma-Aldrich), 450 μM monothioglycerol (Sigma-Aldrich), 5 mg/mL purified BSA (99% purified by crystallization, Sigma-Aldrich), 7 μg/mL insulin (Fujifilm Wako), and penicillin/streptomycin (Invitrogen, Carlsbad, CA, USA). Differentiated hiPSCs were subsequently sorted for CD271 (BioLegend, San Diego, CA, USA) (iNCCs). iNCCs were maintained in CDM supplemented with SB431542, 20 ng/mL epidermal growth factor (EGF) (R&D Systems, Minneapolis, MN, USA), and 20 ng/mL FGF2 (Fujifilm Wako).[96]

### Induction of iMSCs from iNCCs

iNCCs were seeded in cell culture plates coated with fibronectin (Millipore Sigma, Bedford, CA, USA) in CDM supplemented with 10 μM SB431542 and 1 μM CHIR99021. The day before passage, the medium was replaced with MSC induction MEM (Nacalai Tesque, Tokyo, Japan) supplemented with 10% FBS (Nichirei, Tokyo, Japan).[97] The next day, iMSCs were passaged on cell culture dishes using an iMSC induction medium. The cells were induced for 7 days and then passaged. The cells were cultured with mesenchymal stem cell growth medium (MSCGM) (Lonza) and then used as experimental iMSCs.

### Surface and intracellular antigen analysis of iPSCs, iNCCs, and iMSCs

Cell surface antigens for BMMSCs and iMSCs were analyzed using flow cytometry (BD Biosciences, Franklin Lakes, NJ, USA) as described previously.[98] Approximately $1.5 \times 10^5$ cells were incubated with the following conjugated monoclonal antibodies: TRA-1-60/BUV395 (BD Biosciences), TRA-1-81/Alexa Fluor 674, CD271/fluorescein isothiocyanate (FITC), CD90-phycoerythrin (PE)/Cy7, CD105-allophycocyanin (APC), CD73-BV421, CD11b-PE, CD14-PE, CD19-PE, CD34-PE, CD79a-PE, CD45-PE, CD142-PE, and HLA-DR-PE (BioLegend). Nonspecific fluorescence was determined using isotype-matched mouse monoclonal antibodies (BioLegend). Data were analyzed by collecting 10,000 events on a BD FACSAria using FlowJo 8.8.4 software (BD Biosciences). Intracellular antigens for iPSCs and iMSCs were analyzed using immunohistochemistry. Cells were plated on 24-well plates, fixed with 4% paraformaldehyde, and blocked with 2% FBS-0.2% Triton X-100 in phosphate-buffered saline (PBS) for 1 h at room temperature. After blocking, the cells were incubated with anti-Oct3/4 antibody (1:100, Santa Cruz Biotechnology, Dallas, TX, USA) overnight at 4°C and then incubated with Alexa Fluor 568-conjugated anti-mouse immunoglobulin G (IgG; Thermo Fisher Scientific) as secondary antibody at room temperature for 1 h. Fluorescent signals were imaged using an inverted microscope (IX83; Olympus, Tokyo, Japan).

### Mesenchymal differentiation of BMMSCs and iMSCs

Differentiation of MSCs into osteocytes, chondrocytes, and adipocytes was carried out using an MSC osteogenic differentiation medium, chondrogenic differentiation medium (Takara-bio, Shiga, Japan), and the StemPro Adipogenesis Differentiation Kit (Thermo Fisher Scientific), respectively, according to the manufacturer's instructions.

### Cytokine array analysis of BMMSCs and iMSCs

BMMSCs and iMSCs were incubated in MSC medium with or without 10 ng/mL of TNF-α for 2 days, and the culture medium was collected for cytokine array analysis. The relative expression of cytokines and chemokines in the culture medium was quantified using Proteome Profiler Array (Human Cytokine Array, Panel A; R&D Systems), as described previously.[99] To achieve maximum assay sensitivity, the blots were incubated overnight with plasma. Enhanced chemiluminescence incubation was performed for 5 min using the Super Signal West Femto Chemiluminescence Kit (Thermo Scientific Pierce), and the samples were imaged and analyzed using the Image Quant LAS 4000 coupled with Image Quant TL software (GE Healthcare, Chicago, IL, USA) and ImageJ software (NIH, Bethesda, MD, USA).

### Karyotyping analysis

All karyotyping analyses were performed by Chromocenter (Tottori, Japan).

### tMCAO model

All experimental procedures were performed according to guidelines approved by the Nippon Medical School Animal Ethics Committee. Male Sprague-Dawley rats (8 weeks, 250–300 g) were purchased from Sankyo Labo Service (Tokyo, Japan). Rats were fasted overnight before and after surgery and had free access to tap water. Anesthesia was initially induced with 5% isoflurane and then maintained with 1.5% isoflurane in a mixture of 70% $N_2O$ and 30% $O_2$ under spontaneous breathing. A polyethylene PE-50 catheter (BD Biosciences) was inserted into the tail artery to monitor the arterial blood gas condition, blood glucose, and mean arterial blood pressure. The levels were measured immediately before, during, and after ischemia. Rats were subjected to 90-min tMCAO using an intraluminal suture technique.[100] Briefly, the left common, internal carotid, and external carotid arteries were carefully exposed through a midline incision. The common and external carotid arteries were double ligated using 4-0 silk sutures. Focal cerebral ischemia was induced by insertion of 4-0 Medium tMCAO Suture L56 Reusable PK10 (Doccol, Sharon, MA, USA) through the left internal carotid artery for 90 min, which caused reperfusion upon withdrawal. Temporal muscle temperature was maintained at 37°C ± 0.5°C during the procedure.

### Intravenous transplantation of MSCs

A PE-50 catheter was inserted into the tail vein during ischemia. BMMSCs (passage number 4), iMSCs (passage number 1), or vehicle (1 mL of PBS) were injected intravenously through the catheter immediately after I/R. Cell concentration was $1 \times 10^6$ cells in 1 mL of PBS. Cell doses were determined as described previously,[18,19] and the dosing rate was 0.1 mL/min. No immunosuppressive drugs were used.

### Measurement of infarct volumes

To measure infarct volumes, rats were decapitated 3 days after tMCAO (n = 5 for each group). The brains were cut into 2-mm-thick coronal sections and stained with TTC (Fujifilm Wako). The infarct areas were determined separately using ImageJ software (NIH). The infarct area was calculated by subtracting the area of the non-infarcted portion of the ischemic side of the brain from the area of the non-ischemic side of the brain.[101] The infarct areas of each slice were summed separately and multiplied by the interval thickness to obtain infarct volumes.[101]

### Behavioral tests

Neurological symptoms were assessed 3, 7, 14, 28, and 56 days after tMCAO by an observer blinded to the study protocol (n = 8 for each group). Hemiparesis and abnormal posture were evaluated using a previously described scoring system.[102] The right hindlimb of each rat was gently extended with round-tipped forceps, and the flexor response was scored as normal (0), slight deficit (1) moderate deficit (2), or severe deficit (3). For posture assessment, rats were suspended by the tail, and forelimb flexion and body twisting were scored as normal (0), slight twisting (1), marked twisting (2), or marked twisting and forelimb flexion (3). The rotarod test was performed using a rotarod device (model 7750; Ugo Basile, Gemonio, Italy) to examine locomotor coordination ability. The rotation speed of the rod was started at 4 rpm and accelerated to 40 rpm over 5 min with an increase in speed every 30 s. The average reading (in seconds) of three successive trials was obtained for each rat. Preoperative rats that fell repeatedly were placed back onto the rod until they could balance for 150 s. Forelimb grip strength was determined using a grip strength meter (Chatillon DFIS 10; Ametek, Berwyn, PA, USA). The average reading (in newtons) of three successive trials was obtained for each rat. The spontaneous alternation test using the Y-maze apparatus (Muromachi Kikai, Tokyo, Japan) was used to examine spatial working memory.[103,104] Briefly, rats were placed in the start arm and allowed to habituate to the maze environment for 15 min. After 1 h, the rats were placed again in the start arm and allowed to explore the maze freely for 8 min. The number of entries into the arms was counted by an observer blind to the treatment conditions. The percentage of spontaneous alternations was calculated as the ratio of the number of alternations to the total number of arm entries.

### Immunohistochemistry

Rats were deeply anesthetized and transcardially perfused with heparinized saline followed by 4% paraformaldehyde in PBS 3 days after tMCAO (n = 5 for each group). The brains were removed rapidly, and coronal cryosections (12 μm) were cut. The sample sections were incubated with 10% goat serum (Thermo Fisher Scientific) in PBS to block nonspecific reactions, followed by overnight incubation at 4°C with rabbit polyclonal antibodies against Iba-1 (1:125, Fujifilm

Wako), rabbit polyclonal antibody against TNF-α (1:100, Abbiotec, Escondido, CA, USA), mouse monoclonal antibody against 4-HNE (1:250, Japan Institute for the Control of Aging [JaICA], Shizuoka, Japan), and mouse monoclonal antibody against 8-OHdG (1:250, JaICA). Next, the sections were processed with biotinylated goat anti-polyvalent antibody (Thermo Fisher Scientific) at room temperature for 1 h, followed by avidin-biotin-peroxidase complex (Vector Laboratories, Newark, CA, USA) for 30 min. The labeled secondary antibodies were visualized using diaminobenzidine (Vector Laboratories). The protocols for fluorescent staining were as follows. The brain sections were treated with 0.2% Triton X-100 (Sigma-Aldrich) in blocking solution (1:9, UKB80; KAC, Kyoto, Japan), followed by a rabbit polyclonal antibody against TNF-α (1:250; Abcam, Cambridge, UK), a mouse monoclonal antibody against OX42 (CD11b and CD11c) (1:250, Abcam), a mouse monoclonal antibody against GFAP (GA5, 1:250; Cell Signaling Technology, Danvers, MA, USA), a mouse monoclonal antibody against NeuN (Millipore Sima), and a mouse monoclonal antibody against RECA-1 (Abcam) and incubated overnight. The sections were then treated with Alexa Fluor 430 goat anti-rabbit IgG (Molecular Probes, Eugene, OR, USA) or Alexa Fluor 594 goat anti-mouse IgG (Molecular Probes) for 1 h at room temperature under light shielding. The sections were then encapsulated using Vibrance Antifade Mounting Medium with DAPI (Vector Laboratories). To determine the effect of each treatment on neuronal apoptosis and degeneration, the *In Situ* Apoptosis Detection Kit (Takara) or FJC Ready-to-Dilute Staining Kit for Identifying Degenerating Neurons (Biosensis, Thebarton, SA, Australia) commercial kits were used. TUNEL and FJC staining was performed using these kits according to the manufacturer's protocol. Immunofluorescence images were obtained using an all-in-one fluorescence microscope (BZ-X800; Keyence, Osaka, Japan), and otherwise using an optical microscope (Eclipse E500W; Nikon, Tokyo, Japan). Five randomly selected fields of the IBZ adjacent to the ischemic core (0.5 $mm^2$) were counted.

#### Enzyme-linked immunosorbent assay (ELISA)

Concentrations of IL-1β and IL-6 in brain tissue extracts from the ischemic hemisphere were measured using the Rat IL-1β/IL-1F2 Quantikine ELISA Kit and Rat IL-6 Quantikine ELISA Kit (R&D Systems) according to the manufacturer's instructions. Colorimetric absorbance was recorded at a wavelength of 450 nm.

#### SOD activity assay

Total SOD activity in brain tissue extracts from the ischemic hemisphere was measured using a commercial kit (Cayman Chemical, Ann Arbor, MI, USA) with tetrazolium salt for detection of superoxide radicals generated by xanthine oxidase and hypoxanthine. Colorimetric absorbance was measured at a wavelength of 450 nm.

#### Alu-based real-time PCR

The biodistribution and relative amount of engrafted MSCs were determined using Alu-based real-time PCR 3 days after transplantation as described previously.[105] Genomic DNA was prepared from the brain, spleen, lungs, liver, kidneys, and femora of MSC-transplanted rats using the Dneasy Blood & Tissue Kit (QIAGEN, Hilden, Germany). The human Alu-specific primers and TaqMan probe utilized were 5′-GGTGAAACCCCGTCTCTACT-3′ (forward), 5′-GGTTCA AGCGATTCTCCTGC-3′ (reverse), and 5′-FAM-CGCCCGGCTAA TTTTTGTAT-BHQ1-3′ (probe). Real-time PCR for each sample was performed in triplicate using the 7500 Fast Real-Time PCR System (Applied Biosystems, Foster City, CA, USA).

#### Statistical analysis

Data are represented as the mean ± SD or the median and interquartile range (IQR). A one-way analysis of variance, followed by a post hoc Tukey honest significant difference test, was used for comparisons of infarct volume, rotarod test riding time, forelimb grip strength, Y-maze alternation rate, immunohistochemical cell counts, and ELISA data. Additionally, to compare neurological scores, a Kruskal-Wallis test was used. Differences were considered significant at $p < 0.05$. SPSS software v.22 (SPSS, Chicago, IL, USA) was used for all statistical analyses.

## DATA AND CODE AVAILABILITY

The datasets analyzed during this study are available upon reasonable request to the corresponding authors.

## SUPPLEMENTAL INFORMATION

Supplemental information can be found online at https://doi.org/10.1016/j.omtm.2023.07.005.

## ACKNOWLEDGMENTS

We are grateful to Makoto Ikeya (Kyoto University) for cell induction, Atsushi Sakai (Nippon Medical School) for brain sectioning, Masumi Shimizu (Nippon Medical School) for FACS and cell sorting, Yurika Sawa (TechnoPro, Inc., TechnoPro R&D Co.) for histopathological studies, and Kaneka Corp. for BMMSC donation. We would also like to thank the staff of the Laboratory for Clinical Research, Collaborative Research Center for supporting this work. This research was supported by AMED under grant JP22ae0201005 and JSPS KAKENHI grants JP20H03788 and JP18K08981.

## AUTHOR CONTRIBUTIONS

M.A., Y.S., Y.M., and C.N. conceived and designed the research. M.A., Y.S., Y.M., S.T., and Y.Y. performed the experiments. M.A., Y.S., and Y.M. analyzed the data. M.A. and Y.M. wrote the manuscript. Y.M., C.N., Y.N.-K., S.S., M.S., T.O., and K.K. supervised the research. All authors reviewed and edited the manuscript.

## DECLARATION OF INTERESTS

C.N., Y.N-K., and T.O. are co-inventors of intellectual property licensed to Kaneka Corp.

## REFERENCES

1. Bang, O.Y., Lee, J.S., Lee, P.H., and Lee, G. (2005). Autologous mesenchymal stem cell transplantation in stroke patients. Ann. Neurol. *57*, 874–882. https://doi.org/10.1002/ana.20501.

2. Bhatia, V., Gupta, V., Khurana, D., Sharma, R.R., and Khandelwal, N. (2018). Randomized assessment of the safety and efficacy of intra-arterial infusion of autologous stem cells in subacute ischemic stroke. AJNR. Am. J. Neuroradiol. *39*, 899–904. https://doi.org/10.3174/ajnr.A5586.

3. Zhang, R.L., Chopp, M., Zhang, Z.G., Phillips, M.L., Rosenbloom, C.L., Cruz, R., and Manning, A. (1996). E-selectin in focal cerebral ischemia and reperfusion in the rat. J. Cereb. Blood Flow Metab. *16*, 1126–1136. https://doi.org/10.1097/00004647-199611000-00006.

4. Auriel, E., and Bornstein, N.M. (2010). Neuroprotection in acute ischemic stroke–current status. J. Cell Mol. Med. *14*, 2200–2202. https://doi.org/10.1111/j.1582-4934.2010.01135.x.

5. Kobayashi, S., Fukuma, S., Ikenoue, T., Fukuhara, S., and Kobayashi, S. (2019). Effect of edaravone on neurological symptoms in real-world patients with acute ischemic stroke. Stroke *50*, 1805–1811. https://doi.org/10.1161/STROKEAHA.118.024351.

6. Song, M., Lee, J.H., Bae, J., Bu, Y., and Kim, E.C. (2017). Human dental pulp stem cells are more effective than human bone marrow-derived mesenchymal stem cells in cerebral ischemic injury. Cell Transplant. *26*, 1001–1016. https://doi.org/10.3727/096368916X694391.

7. Kawabori, M., Kuroda, S., Ito, M., Shichinohe, H., Houkin, K., Kuge, Y., and Tamaki, N. (2013). Timing and cell dose determine therapeutic effects of bone marrow stromal cell transplantation in rat model of cerebral infarct. Neuropathology *33*, 140–148. https://doi.org/10.1111/j.1440-1789.2012.01335.x.

8. Wang, L.Q., Lin, Z.Z., Zhang, H.X., Shao, B., Xiao, L., Jiang, H.G., Zhuge, Q.C., Xie, L.K., Wang, B., Su, D.M., and Jin, K.L. (2014). Timing and dose regimens of marrow mesenchymal stem cell transplantation affect the outcomes and neuroinflammatory response after ischemic stroke. CNS Neurosci. Ther. *20*, 317–326. https://doi.org/10.1111/cns.12216.

9. Kwak, K.A., Kwon, H.B., Lee, J.W., and Park, Y.S. (2018). Current Perspectives regarding stem cell-based therapy for ischemic stroke. Curr. Pharm. Des. *24*, 3332–3340. https://doi.org/10.2174/1381612824666180604111806.

10. Horita, Y., Honmou, O., Harada, K., Houkin, K., Hamada, H., and Kocsis, J.D. (2006). Intravenous administration of glial cell line-derived neurotrophic factor gene-modified human mesenchymal stem cells protects against injury in a cerebral ischemia model in the adult rat. J. Neurosci. Res. *84*, 1495–1504. https://doi.org/10.1002/jnr.21056.

11. Oh, S.H., Choi, C., Noh, J.E., Lee, N., Jeong, Y.W., Jeon, I., Shin, J.M., Kim, J.H., Kim, H.J., Lee, J.M., et al. (2018). Interleukin-1 receptor antagonist-mediated neuroprotection by umbilical cord-derived mesenchymal stromal cells following transplantation into a rodent stroke model. Exp. Mol. Med. *50*, 1–12. https://doi.org/10.1038/s12276-018-0041-1.

12. Lü, C., Liu, Q., and Zeng, X. (2017). [Effects of interleukin 10 gene modified bone marrow mesenchymal stem cells on expression of inflammatory cytokines and neuronal apoptosis in rats after cerebral ischemia reperfusion injury]. Zhongguo Xiu Fu Chong Jian Wai Ke Za Zhi *31*, 240–245. https://doi.org/10.7507/1002-1892.201605095.

13. Onda, T., Honmou, O., Harada, K., Houkin, K., Hamada, H., and Kocsis, J.D. (2008). Therapeutic benefits by human mesenchymal stem cells (hMSCs) and Ang-1 gene-modified hMSCs after cerebral ischemia. J. Cereb. Blood Flow Metab. *28*, 329–340. https://doi.org/10.1038/sj.jcbfm.9600527.

14. Ukai, R., Honmou, O., Harada, K., Houkin, K., Hamada, H., and Kocsis, J.D. (2007). Mesenchymal stem cells derived from peripheral blood protects against ischemia. J. Neurotrauma *24*, 508–520. https://doi.org/10.1089/neu.2006.0161.

15. Omori, Y., Honmou, O., Harada, K., Suzuki, J., Houkin, K., and Kocsis, J.D. (2008). Optimization of a therapeutic protocol for intravenous injection of human mesenchymal stem cells after cerebral ischemia in adult rats. Brain Res. *1236*, 30–38. https://doi.org/10.1016/j.brainres.2008.07.116.

16. Bao, X., Feng, M., Wei, J., Han, Q., Zhao, H., Li, G., Zhu, Z., Xing, H., An, Y., Qin, C., et al. (2011). Transplantation of Flk-1+ human bone marrow-derived mesenchymal stem cells promotes angiogenesis and neurogenesis after cerebral ischemia in rats. Eur. J. Neurosci. *34*, 87–98. https://doi.org/10.1111/j.1460-9568.2011.07733.x.

17. Hao, L., Zou, Z., Tian, H., Zhang, Y., Zhou, H., and Liu, L. (2014). Stem cell-based therapies for ischemic stroke. BioMed Res. Int. *2014*, 468748. https://doi.org/10.1155/2014/468748.

18. Nakajima, M., Nito, C., Sowa, K., Suda, S., Nishiyama, Y., Nakamura-Takahashi, A., Nitahara-Kasahara, Y., Imagawa, K., Hirato, T., Ueda, M., et al. (2017). Mesenchymal stem cells overexpressing interleukin-10 promote neuroprotection in experimental acute ischemic stroke. Mol. Ther. Methods Clin. Dev. *6*, 102–111. https://doi.org/10.1016/j.omtm.2017.06.005.

19. Sowa, K., Nito, C., Nakajima, M., Suda, S., Nishiyama, Y., Sakamoto, Y., Nitahara-Kasahara, Y., Nakamura-Takahashi, A., Ueda, M., Kimura, K., and Okada, T. (2018). Impact of dental pulp stem cells overexpressing hepatocyte growth factor after cerebral ischemia/reperfusion in rats. Mol. Ther. Methods Clin. Dev. *10*, 281–290. https://doi.org/10.1016/j.omtm.2018.07.009.

20. Shichinohe, H., Kawabori, M., Iijima, H., Teramoto, T., Abumiya, T., Nakayama, N., Kazumata, K., Terasaka, S., Arato, T., and Houkin, K. (2017). Research on advanced intervention using novel bone marrow stem cell (RAINBOW): a study protocol for a phase I, open-label, uncontrolled, dose-response trial of autologous bone marrow stromal cell transplantation in patients with acute ischemic stroke. BMC Neurol. *17*, 179. https://doi.org/10.1186/s12883-017-0955-6.

21. Zaim, M., Karaman, S., Cetin, G., and Isik, S. (2012). Donor age and long-term culture affect differentiation and proliferation of human bone marrow mesenchymal stem cells. Ann. Hematol. *91*, 1175–1186. https://doi.org/10.1007/s00277-012-1438-x.

22. Trounson, A., and DeWitt, N.D. (2016). Pluripotent stem cells progressing to the clinic. Nat. Rev. Mol. Cell Biol. *17*, 194–200. https://doi.org/10.1038/nrm.2016.10.

23. Liu, Z., Tang, Y., Lü, S., Zhou, J., Du, Z., Duan, C., Li, Z., and Wang, C. (2013). The tumourigenicity of iPS cells and their differentiated derivates. J. Cell Mol. Med. *17*, 782–791. https://doi.org/10.1111/jcmm.12062.

24. Yamada, D., Nakamura, M., Takao, T., Takihira, S., Yoshida, A., Kawai, S., Miura, A., Ming, L., Yoshitomi, H., Gozu, M., et al. (2021). Induction and expansion of human PRRX1(+) limb-bud-like mesenchymal cells from pluripotent stem cells. Nat. Biomed. Eng. *5*, 926–940. https://doi.org/10.1038/s41551-021-00778-x.

25. Tan, J.J., Guyette, J.P., Miki, K., Xiao, L., Kaur, G., Wu, T., Zhu, L., Hansen, K.J., Ling, K.H., Milan, D.J., and Ott, H.C. (2021). Human iPS-derived pre-epicardial cells direct cardiomyocyte aggregation expansion and organization in vitro. Nat. Commun. *12*, 4997. https://doi.org/10.1038/s41467-021-24921-z.

26. Taguchi, A., Kaku, Y., Ohmori, T., Sharmin, S., Ogawa, M., Sasaki, H., and Nishinakamura, R. (2014). Redefining the in vivo origin of metanephric nephron progenitors enables generation of complex kidney structures from pluripotent stem cells. Cell Stem Cell *14*, 53–67. https://doi.org/10.1016/j.stem.2013.11.010.

27. Fukuta, M., Nakai, Y., Kirino, K., Nakagawa, M., Sekiguchi, K., Nagata, S., Matsumoto, Y., Yamamoto, T., Umeda, K., Heike, T., et al. (2014). Derivation of mesenchymal stromal cells from pluripotent stem cells through a neural crest lineage using small molecule compounds with defined media. PLoS One *9*, e112291. https://doi.org/10.1371/journal.pone.0112291.

28. Ouchi, T., Morikawa, S., Shibata, S., Fukuda, K., Okuno, H., Fujimura, T., Kuroda, T., Ohyama, M., Akamatsu, W., Nakagawa, T., and Okano, H. (2016). LNGFR(+) THY-1(+) human pluripotent stem cell-derived neural crest-like cells have the potential to develop into mesenchymal stem cells. Differentiation. *92*, 270–280. https://doi.org/10.1016/j.diff.2016.04.003.

29. Lian, Q., Lye, E., Suan Yeo, K., Khia Way Tan, E., Salto-Tellez, M., Liu, T.M., Palanisamy, N., El Oakley, R.M., Lee, E.H., Lim, B., and Lim, S.K. (2007). Derivation of clinically compliant MSCs from CD105+, CD24- differentiated human ESCs. Stem Cell. *25*, 425–436. https://doi.org/10.1634/stemcells.2006-0420.

30. Lian, Q., Zhang, Y., Zhang, J., Zhang, H.K., Wu, X., Zhang, Y., Lam, F.F.Y., Kang, S., Xia, J.C., Lai, W.H., et al. (2010). Functional mesenchymal stem cells derived from human induced pluripotent stem cells attenuate limb ischemia in mice. Circulation *121*, 1113–1123. https://doi.org/10.1161/circulationaha.109.898312.

31. Soontararak, S., Chow, L., Johnson, V., Coy, J., Wheat, W., Regan, D., and Dow, S. (2018). Mesenchymal stem cells (MSC) derived from induced pluripotent stem cells (iPSC) equivalent to adipose-derived MSC in promoting intestinal healing and microbiome normalization in mouse inflammatory bowel disease model. Stem Cells Transl. Med. *7*, 456–467. https://doi.org/10.1002/sctm.17-0305.

32. Yun, Y.I., Park, S.Y., Lee, H.J., Ko, J.H., Kim, M.K., Wee, W.R., Reger, R.L., Gregory, C.A., Choi, H., Fulcher, S.F., et al. (2017). Comparison of the anti-inflammatory effects of induced pluripotent stem cell-derived and bone marrow-derived

mesenchymal stromal cells in a murine model of corneal injury. Cytotherapy *19*, 28–35. https://doi.org/10.1016/j.jcyt.2016.10.007.

33. Chen, K.H., Lin, K.C., Wallace, C.G., Li, Y.C., Shao, P.L., Chiang, J.Y., Sung, P.H., and Yip, H.K. (2019). Human induced pluripotent stem cell-derived mesenchymal stem cell therapy effectively reduced brain infarct volume and preserved neurological function in rat after acute intracranial hemorrhage. Am. J. Transl. Res. *11*, 6232–6248.

34. Xia, Y., Ling, X., Hu, G., Zhu, Q., Zhang, J., Li, Q., Zhao, B., Wang, Y., and Deng, Z. (2020). Small extracellular vesicles secreted by human iPSC-derived MSC enhance angiogenesis through inhibiting STAT3-dependent autophagy in ischemic stroke. Stem Cell Res. Ther. *11*, 313. https://doi.org/10.1186/s13287-020-01834-0.

35. Abdal Dayem, A., Lee, S.B., Kim, K., Lim, K.M., Jeon, T.I., Seok, J., and Cho, A.S.G. (2019). Production of Mesenchymal Stem Cells Through Stem Cell Reprogramming. Int. J. Mol. Sci. *20*, 1922. https://doi.org/10.3390/ijms20081922.

36. Lv, W., Li, W.Y., Xu, X.Y., Jiang, H., and Bang, O.Y. (2015). Bone marrow mesenchymal stem cells transplantation promotes the release of endogenous erythropoietin after ischemic stroke. Neural Regen. Res. *10*, 1265–1270. https://doi.org/10.4103/1673-5374.162759.

37. Du, S., Guan, J., Mao, G., Liu, Y., Ma, S., Bao, X., Gao, J., Feng, M., Li, G., Ma, W., et al. (2014). Intra-arterial delivery of human bone marrow mesenchymal stem cells is a safe and effective way to treat cerebral ischemia in rats. Cell Transplant. *23*, S73–S82. S73–82. https://doi.org/10.3727/096368914x685023.

38. Wei, J.J., Zeng, L.F., Fan, X.T., Wang, Y., Ma, W.B., Li, G.L., Dou, W.C., Zhang, Z.X., Li, S.F., Feng, M., et al. (2007). [Treatment of stroke in rats with bone marrow mesenchymal stem cells]. Zhonghua Yixue Zazhi *87*, 184–189.

39. He, B., Yao, Q., Liang, Z., Lin, J., Xie, Y., Li, S., Wu, G., Yang, Z., and Xu, P. (2016). The dose of intravenously transplanted bone marrow stromal cells determines the therapeutic effect on vascular remodeling in a rat model of ischemic stroke. Cell Transplant. *25*, 2173–2185. https://doi.org/10.3727/096368916x692627.

40. Bao, X., Wei, J., Feng, M., Lu, S., Li, G., Dou, W., Ma, W., Ma, S., An, Y., Qin, C., et al. (2011). Transplantation of human bone marrow-derived mesenchymal stem cells promotes behavioral recovery and endogenous neurogenesis after cerebral ischemia in rats. Brain Res. *1367*, 103–113. https://doi.org/10.1016/j.brainres.2010.10.063.

41. Li, Z., Ye, H., Cai, X., Sun, W., He, B., Yang, Z., and Xu, P. (2019). Bone marrow-mesenchymal stem cells modulate microglial activation in the peri-infarct area in rats during the acute phase of stroke. Brain Res. Bull. *153*, 324–333. https://doi.org/10.1016/j.brainresbull.2019.10.001.

42. Lee, J.S., Hong, J.M., Moon, G.J., Lee, P.H., Ahn, Y.H., and Bang, O.Y.; STARTING collaborators (2010). A long-term follow-up study of intravenous autologous mesenchymal stem cell transplantation in patients with ischemic stroke. Stem Cell. *28*, 1099–1106. https://doi.org/10.1002/stem.430.

43. Honmou, O., Houkin, K., Matsunaga, T., Niitsu, Y., Ishiai, S., Onodera, R., Waxman, S.G., and Kocsis, J.D. (2011). Intravenous administration of auto serum-expanded autologous mesenchymal stem cells in stroke. Brain *134* (Pt 6), 1790–1807. https://doi.org/10.1093/brain/awr063.

44. Jaillard, A., Hommel, M., Moisan, A., Zeffiro, T.A., Favre-Wiki, I.M., Barbieux-Guillot, M., Vadot, W., Marcel, S., Lamalle, L., Grand, S., et al. (2020). Autologous mesenchymal stem cells improve motor recovery in subacute ischemic stroke: a randomized clinical trial. Transl. Stroke Res. *11*, 910–923. https://doi.org/10.1007/s12975-020-00787-z.

45. Costa, L.A., Eiro, N., Fraile, M., Gonzalez, L.O., Saá, J., Garcia-Portabella, P., Vega, B., Schneider, J., and Vizoso, F.J. (2021). Functional heterogeneity of mesenchymal stem cells from natural niches to culture conditions: implications for further clinical uses. Cell. Mol. Life Sci. *78*, 447–467. https://doi.org/10.1007/s00018-020-03600-0.

46. Siegel, G., Kluba, T., Hermanutz-Klein, U., Bieback, K., Northoff, H., and Schäfer, R. (2013). Phenotype, donor age and gender affect function of human bone marrow-derived mesenchymal stromal cells. BMC Med. *11*, 146. https://doi.org/10.1186/1741-7015-11-146.

47. Xu, L., Liu, Y., Sun, Y., Wang, B., Xiong, Y., Lin, W., Wei, Q., Wang, H., He, W., Wang, B., and Li, G. (2017). Tissue source determines the differentiation potentials of mesenchymal stem cells: a comparative study of human mesenchymal stem cells from bone marrow and adipose tissue. Stem Cell Res. Ther. *8*, 275. https://doi.org/10.1186/s13287-017-0716-x.

48. Stenderup, K., Justesen, J., Clausen, C., and Kassem, M. (2003). Aging is associated with decreased maximal life span and accelerated senescence of bone marrow stromal cells. Bone *33*, 919–926. https://doi.org/10.1016/j.bone.2003.07.005.

49. Neri, S., and Borzì, R.M. (2020). Molecular Mechanisms Contributing to Mesenchymal Stromal Cell Aging. Biomolecules *10*, 340. https://doi.org/10.3390/biom10020340.

50. Liu, J., Ding, Y., Liu, Z., and Liang, X. (2020). Senescence in Mesenchymal Stem Cells: Functional Alterations, Molecular Mechanisms, and Rejuvenation Strategies. Front. Cell Dev. Biol. *8*, 258. https://doi.org/10.3389/fcell.2020.00258.

51. Dominici, M., Le Blanc, K., Mueller, I., Slaper-Cortenbach, I., Marini, F.C., Krause, D.S., Deans, R.J., Keating, A., Prockop, D.J., and Horwitz, E.M. (2006). Minimal criteria for defining multipotent mesenchymal stromal cells. The International Society for Cellular Therapy position statement. Cytotherapy *8*, 315–317. https://doi.org/10.1080/14653240600855905.

52. Kang, R., Zhou, Y., Tan, S., Zhou, G., Aagaard, L., Xie, L., Bünger, C., Bolund, L., and Luo, Y. (2015). Mesenchymal stem cells derived from human induced pluripotent stem cells retain adequate osteogenicity and chondrogenicity but less adipogenicity. Stem Cell Res. Ther. *6*, 144. https://doi.org/10.1186/s13287-015-0137-7.

53. Zou, L., Luo, Y., Chen, M., Wang, G., Ding, M., Petersen, C.C., Kang, R., Dagnaes-Hansen, F., Zeng, Y., Lv, N., et al. (2013). A simple method for deriving functional MSCs and applied for osteogenesis in 3D scaffolds. Sci. Rep. *3*, 2243. https://doi.org/10.1038/srep02243.

54. Zhang, Y., Liang, X., Liao, S., Wang, W., Wang, J., Li, X., Ding, Y., Liang, Y., Gao, F., Yang, M., et al. (2015). potent paracrine effects of human induced pluripotent stem cell-derived mesenchymal stem cells attenuate doxorubicin-induced cardiomyopathy. Sci. Rep. *5*, 11235. https://doi.org/10.1038/srep11235.

55. Obara, C., Takizawa, K., Tomiyama, K., Hazawa, M., Saotome-Nakamura, A., Gotoh, T., Yasuda, T., and Tajima, K. (2016). Differentiation and molecular properties of mesenchymal stem cells derived from murine induced pluripotent stem cells derived on gelatin or collagen. Stem Cells Int. *2016*, 9013089. https://doi.org/10.1155/2016/9013089.

56. Xu, M., Shaw, G., Murphy, M., and Barry, F. (2019). Induced pluripotent stem cell-derived mesenchymal stromal cells are functionally and genetically different from bone marrow-derived mesenchymal stromal cells. Stem Cell. *37*, 754–765. https://doi.org/10.1002/stem.2993.

57. Diederichs, S., and Tuan, R.S. (2014). Functional comparison of human-induced pluripotent stem cell-derived mesenchymal cells and bone marrow-derived mesenchymal stromal cells from the same donor. Stem Cells Dev. *23*, 1594–1610. https://doi.org/10.1089/scd.2013.0477.

58. Hynes, K., Menicanin, D., Mrozik, K., Gronthos, S., and Bartold, P.M. (2014). Generation of functional mesenchymal stem cells from different induced pluripotent stem cell lines. Stem Cells Dev. *23*, 1084–1096. https://doi.org/10.1089/scd.2013.0111.

59. Frobel, J., Hemeda, H., Lenz, M., Abagnale, G., Joussen, S., Denecke, B., Sarić, T., Zenke, M., and Wagner, W. (2014). Epigenetic rejuvenation of mesenchymal stromal cells derived from induced pluripotent stem cells. Stem Cell Rep. *3*, 414–422. https://doi.org/10.1016/j.stemcr.2014.07.003.

60. Ahfeldt, T., Schinzel, R.T., Lee, Y.K., Hendrickson, D., Kaplan, A., Lum, D.H., Camahort, R., Xia, F., Shay, J., Rhee, E.P., et al. (2012). Programming human pluripotent stem cells into white and brown adipocytes. Nat. Cell Biol. *14*, 209–219. https://doi.org/10.1038/ncb2411.

61. Spitzhorn, L.S., Megges, M., Wruck, W., Rahman, M.S., Otte, J., Degistirici, Ö., Meisel, R., Sorg, R.V., Oreffo, R.O.C., and Adjaye, J. (2019). Human iPSC-derived MSCs (iMSCs) from aged individuals acquire a rejuvenation signature. Stem Cell Res. Ther. *10*, 100. https://doi.org/10.1186/s13287-019-1209-x.

62. Zhu, Y., Wang, Y., Zhao, B., Niu, X., Hu, B., Li, Q., Zhang, J., Ding, J., Chen, Y., and Wang, Y. (2017). Comparison of exosomes secreted by induced pluripotent stem cell-derived mesenchymal stem cells and synovial membrane-derived mesenchymal stem cells for the treatment of osteoarthritis. Stem Cell Res. Ther. *8*, 64. https://doi.org/10.1186/s13287-017-0510-9.

63. Tang, M., Chen, W., Liu, J., Weir, M.D., Cheng, L., and Xu, H.H.K. (2014). Human induced pluripotent stem cell-derived mesenchymal stem cell seeding on calcium

phosphate scaffold for bone regeneration. Tissue Eng. Part A *207-8*, 1295–1305. https://doi.org/10.1089/ten.TEA.2013.0211.

64. Zhao, Q., Gregory, C.A., Lee, R.H., Reger, R.L., Qin, L., Hai, B., Park, M.S., Yoon, N., Clough, B., McNeill, E., et al. (2015). MSCs derived from iPSCs with a modified protocol are tumor-tropic but have much less potential to promote tumors than bone marrow MSCs. Proc. Natl. Acad. Sci. USA *112*, 530–535. https://doi.org/10.1073/pnas.1423008112.

65. Hai, B., Shigemoto-Kuroda, T., Zhao, Q., Lee, R.H., and Liu, F. (2018). Inhibitory Effects of iPSC-MSCs and their extracellular vesicles on the onset of sialadenitis in a mouse model of Sjögren's syndrome. Stem Cells Int. *2018*, 2092315. https://doi.org/10.1155/2018/2092315.

66. Mizuno, M., Ozeki, N., and Sekiya, I. (2022). Safety of using cultured cells with trisomy 7 in cell therapy for treating osteoarthritis. Regen. Ther. Jun *17*, 81–86. https://doi.org/10.1016/j.reth.2022.06.003.

67. Chen, Z., Han, X., Ouyang, X., Fang, J., Huang, X., and Wei, H. (2019). Transplantation of induced pluripotent stem cell-derived mesenchymal stem cells improved erectile dysfunction induced by cavernous nerve injury. Theranostics *9*, 6354–6368. https://doi.org/10.7150/thno.34008.

68. Katsha, A.M., Ohkouchi, S., Xin, H., Kanehira, M., Sun, R., Nukiwa, T., and Saijo, Y. (2011). Paracrine factors of multipotent stromal cells ameliorate lung injury in an elastase-induced emphysema model. Mol. Ther. *19*, 196–203. https://doi.org/10.1038/mt.2010.192.

69. Mitkari, B., Kerkelä, E., Nystedt, J., Korhonen, M., Mikkonen, V., Huhtala, T., and Jolkkonen, J. (2013). Intra-arterial infusion of human bone marrow-derived mesenchymal stem cells results in transient localization in the brain after cerebral ischemia in rats. Exp. Neurol. *239*, 158–162. https://doi.org/10.1016/j.expneurol.2012.09.018.

70. Wu, T., Lang, J., Sun, X., Zhang, B., Liu, Y., and An, R. (2013). Monitoring bone marrow stem cells with a reporter gene system in experimental middle cerebral artery occlusion rat models. J. Nucl. Med. *54*, 984–989. https://doi.org/10.2967/jnumed.112.109280.

71. Gu, Y., He, M., Zhou, X., Liu, J., Hou, N., Bin, T., Zhang, Y., Li, T., and Chen, J. (2016). Endogenous IL-6 of mesenchymal stem cell improves behavioral outcome of hypoxic-ischemic brain damage neonatal rats by supressing apoptosis in astrocyte. Sci. Rep. *6*, 18587. https://doi.org/10.1038/srep18587.

72. Zhao, M.Z., Nonoguchi, N., Ikeda, N., Watanabe, T., Furutama, D., Miyazawa, D., Funakoshi, H., Kajimoto, Y., Nakamura, T., Dezawa, M., et al. (2006). Novel therapeutic strategy for stroke in rats by bone marrow stromal cells and ex vivo HGF gene transfer with HSV-1 vector. J. Cereb. Blood Flow Metab. *26*, 1176–1188. https://doi.org/10.1038/sj.jcbfm.9600273.

73. Kurozumi, K., Nakamura, K., Tamiya, T., Kawano, Y., Ishii, K., Kobune, M., Hirai, S., Uchida, H., Sasaki, K., Ito, Y., et al. (2005). Mesenchymal stem cells that produce neurotrophic factors reduce ischemic damage in the rat middle cerebral artery occlusion model. Mol. Ther. *11*, 96–104. https://doi.org/10.1016/j.ymthe.2004.09.020.

74. Li, Y., Chen, J., Chen, X.G., Wang, L., Gautam, S.C., Xu, Y.X., Katakowski, M., Zhang, L.J., Lu, M., Janakiraman, N., and Chopp, M. (2002). Human marrow stromal cell therapy for stroke in rat: neurotrophins and functional recovery. Neurology *59*, 514–523. https://doi.org/10.1212/wnl.59.4.514.

75. Cheng, X., Wang, H., Zhang, X., Zhao, S., Zhou, Z., Mu, X., Zhao, C., and Teng, W. (2017). The role of SDF-1/CXCR4/CXCR7 in neuronal regeneration after cerebral ischemia. Front. Neurosci. *11*, 590. https://doi.org/10.3389/fnins.2017.00590.

76. Mao, W., Yi, X., Qin, J., Tian, M., and Jin, G. (2014). CXCL12 inhibits cortical neuron apoptosis by increasing the ratio of Bcl-2/Bax after traumatic brain injury. Int. J. Neurosci. *124*, 281–290. https://doi.org/10.3109/00207454.2013.838236.

77. Wang, Q., Xu, Y., Chen, J.C., Qin, Y.Y., Liu, M., Liu, Y., Xie, M.J., Yu, Z.Y., Zhu, Z., and Wang, W. (2012). Stromal cell-derived factor 1α decreases β-amyloid deposition in Alzheimer's disease mouse model. Brain Res. *1459*, 15–26. https://doi.org/10.1016/j.brainres.2012.04.011.

78. Yellowley, C. (2013). CXCL12/CXCR4 signaling and other recruitment and homing pathways in fracture repair. BoneKEy Rep. *2*, 300. https://doi.org/10.1038/bonekey.2013.34.

79. Brick, R.M., Sun, A.X., and Tuan, R.S. (2018). Neurotrophically induced mesenchymal progenitor cells derived from induced pluripotent stem cells enhance neuritogenesis via neurotrophin and cytokine production. Stem Cells Transl. Med. *7*, 45–58. https://doi.org/10.1002/sctm.17-0108.

80. Jin, K., Zhu, Y., Sun, Y., Mao, X.O., Xie, L., and Greenberg, D.A. (2002). Vascular endothelial growth factor (VEGF) stimulates neurogenesis in vitro and in vivo. Proc. Natl. Acad. Sci. USA *99*, 11946–11950. https://doi.org/10.1073/pnas.182296499.

81. Bao, X.J., Liu, F.Y., Lu, S., Han, Q., Feng, M., Wei, J.J., Li, G.L., Zhao, R.C.H., and Wang, R.Z. (2013). Transplantation of Flk-1+ human bone marrow-derived mesenchymal stem cells promotes behavioral recovery and anti-inflammatory and angiogenesis effects in an intracerebral hemorrhage rat model. Int. J. Mol. Med. *31*, 1087–1096. https://doi.org/10.3892/ijmm.2013.1290.

82. Liu, N., Chen, R., Du, H., Wang, J., Zhang, Y., and Wen, J. (2009). Expression of IL-10 and TNF-alpha in rats with cerebral infarction after transplantation with mesenchymal stem cells. Cell. Mol. Immunol. *6*, 207–213. https://doi.org/10.1038/cmi.2009.28.

83. Calió, M.L., Marinho, D.S., Ko, G.M., Ribeiro, R.R., Carbonel, A.F., Oyama, L.M., Ormanji, M., Guirao, T.P., Calió, P.L., Reis, L.A., et al. (2014). Transplantation of bone marrow mesenchymal stem cells decreases oxidative stress, apoptosis, and hippocampal damage in brain of a spontaneous stroke model. Free Radic. Biol. Med. *70*, 141–154. https://doi.org/10.1016/j.freeradbiomed.2014.01.024.

84. Jeong, C.H., Kim, S.M., Lim, J.Y., Ryu, C.H., Jun, J.A., and Jeun, S.S. (2014). Mesenchymal stem cells expressing brain-derived neurotrophic factor enhance endogenous neurogenesis in an ischemic stroke model. BioMed Res. Int. *2014*, 129145. https://doi.org/10.1155/2014/129145.

85. Doeppner, T.R., Herz, J., Görgens, A., Schlechter, J., Ludwig, A.K., Radtke, S., de Miroschedji, K., Horn, P.A., Giebel, B., and Hermann, D.M. (2015). Extracellular vesicles improve post-stroke neuroregeneration and prevent postischemic immunosuppression. Stem Cells transl. med. *4*, 1131–1143. https://doi.org/10.5966/sctm.2015-0078.

86. Sammali, E., Alia, C., Vegliante, G., Colombo, V., Giordano, N., Pischiutta, F., Boncoraglio, G.B., Barilani, M., Lazzari, L., Caleo, M., et al. (2017). Intravenous infusion of human bone marrow mesenchymal stromal cells promotes functional recovery and neuroplasticity after ischemic stroke in mice. Sci. Rep. *7*, 6962. https://doi.org/10.1038/s41598-017-07274-w.

87. Xu, R., Bai, Y., Min, S., Xu, X., Tang, T., and Ju, S. (2020). In vivo monitoring and assessment of exogenous mesenchymal stem cell-derived exosomes in mice with ischemic stroke by molecular imaging. Int. J. Nanomedicine *15*, 9011–9023. https://doi.org/10.2147/ijn.s271519.

88. Xin, H., Li, Y., Cui, Y., Yang, J.J., Zhang, Z.G., and Chopp, M. (2013). Systemic administration of exosomes released from mesenchymal stromal cells promote functional recovery and neurovascular plasticity after stroke in rats. J. Cereb. Blood Flow Metab. *33*, 1711–1715. https://doi.org/10.1038/jcbfm.2013.152.

89. Giuliani, M., Oudrhiri, N., Noman, Z.M., Vernochet, A., Chouaib, S., Azzarone, B., Durrbach, A., and Bennaceur-Griscelli, A. (2011). Human mesenchymal stem cells derived from induced pluripotent stem cells down-regulate NK-cell cytolytic machinery. Blood *118*, 3254–3262. https://doi.org/10.1182/blood-2010-12-325324.

90. Moll, G., Ankrum, J.A., Olson, S.D., and Nolta, J.A. (2022). Improved MSC minimal criteria to maximize patient safety: A call to embrace tissue factor and hemocompatibility assessment of MSC Products. Stem Cells Transl. Med. *11*, 2–13. https://doi.org/10.1093/stcltm/szab005.

91. Moll, G., Drzeniek, N., Kamhieh-Milz, J., Geissler, S., Volk, H.D., and Reinke, P. (2020). MSC therapies for COVID-19: Importance of patient coagulopathy, thromboprophylaxis, cell product quality and mode of delivery for treatment safety and efficacy. Front. Immunol. *11*, 1091. https://doi.org/10.3389/fimmu.2020.01091.

92. Bui, H.T.H., Nguyen, L.T., and Than, U.T.T. (2021). Influences of xeno-free media on mesenchymal stem cell expansion for clinical application. Tissue Eng. Regen. Med. *18*, 15–23. https://doi.org/10.1007/s13770-020-00306-z.

93. Nagasaki, K., Nakashima, A., Tamura, R., Ishiuchi, N., Honda, K., Ueno, T., Doi, S., Kato, Y., and Masaki, T. (2021). Mesenchymal stem cells cultured in serum-free medium ameliorate experimental peritoneal fibrosis. Stem Cell Res. Ther. *12*, 203. https://doi.org/10.1186/s13287-021-02273-1.

94. Ono, M., Hamada, Y., Horiuchi, Y., Matsuo-Takasaki, M., Imoto, Y., Satomi, K., Arinami, T., Hasegawa, M., Fujioka, T., Nakamura, Y., and Noguchi, E. (2012).

Generation of induced pluripotent stem cells from human nasal epithelial cells using a Sendai virus vector. PLoS One *7*, e42855. https://doi.org/10.1371/journal.pone.0042855.

95. Wataya, T., Ando, S., Muguruma, K., Ikeda, H., Watanabe, K., Eiraku, M., Kawada, M., Takahashi, J., Hashimoto, N., and Sasai, Y. (2008). Minimization of exogenous signals in ES cell culture induces rostral hypothalamic differentiation. Proc. Natl. Acad. Sci. USA *105*, 11796–11801. https://doi.org/10.1073/pnas.0803078105.

96. Colleoni, S., Galli, C., Giannelli, S.G., Armentero, M.T., Blandini, F., Broccoli, V., and Lazzari, G. (2010). Long-term culture and differentiation of CNS precursors derived from anterior human neural rosettes following exposure to ventralizing factors. Exp. Cell Res. *316*, 1148–1158. https://doi.org/10.1016/j.yexcr.2010.02.013.

97. Menendez, L., Yatskievych, T.A., Antin, P.B., and Dalton, S. (2011). Wnt signaling and a Smad pathway blockade direct the differentiation of human pluripotent stem cells to multipotent neural crest cells. Proc. Natl. Acad. Sci. USA *108*, 19240–19245. https://doi.org/10.1073/pnas.1113746108.

98. Nitahara-Kasahara, Y., Hayashita-Kinoh, H., Ohshima-Hosoyama, S., Okada, H., Wada-Maeda, M., Nakamura, A., Okada, T., and Takeda, S. (2012). Long-term engraftment of multipotent mesenchymal stromal cells that differentiate to form myogenic cells in dogs with Duchenne muscular dystrophy. Mol. Ther. *20*, 168–177. https://doi.org/10.1038/mt.2011.181.

99. Nitahara-Kasahara, Y., Hayashita-Kinoh, H., Chiyo, T., Nishiyama, A., Okada, H., Takeda, S., and Okada, T. (2014). Dystrophic mdx mice develop severe cardiac and respiratory dysfunction following genetic ablation of the anti-inflammatory cytokine IL-10. Hum. Mol. Genet. *23*, 3990–4000. https://doi.org/10.1093/hmg/ddu113.

100. Nito, C., Ueda, M., Inaba, T., Katsura, K.I., and Katayama, Y. (2011). FK506 ameliorates oxidative damage and protects rat brain following transient focal cerebral ischemia. Neurol. Res. *33*, 881–889. https://doi.org/10.1179/1743132811y.0000000019.

101. Lin, T.N., He, Y.Y., Wu, G., Khan, M., and Hsu, C.Y. (1993). Effect of brain edema on infarct volume in a focal cerebral ischemia model in rats. Stroke *24*, 117–121. https://doi.org/10.1161/01.str.24.1.117.

102. Yonemori, F., Yamaguchi, T., Yamada, H., and Tamura, A. (1998). Evaluation of a motor deficit after chronic focal cerebral ischemia in rats. J. Cereb. Blood Flow Metab. *18*, 1099–1106. https://doi.org/10.1097/00004647-199810000-00006.

103. McNay, E.C., Fries, T.M., and Gold, P.E. (2000). Decreases in rat extracellular hippocampal glucose concentration associated with cognitive demand during a spatial task. Proc. Natl. Acad. Sci. USA *97*, 2881–2885. https://doi.org/10.1073/pnas.050583697.

104. Kanamaru, T., Kamimura, N., Yokota, T., Nishimaki, K., Iuchi, K., Lee, H., Takami, S., Akashiba, H., Shitaka, Y., Ueda, M., et al. (2015). Intravenous transplantation of bone marrow-derived mononuclear cells prevents memory impairment in transgenic mouse models of Alzheimer's disease. Brain Res. *1605*, 49–58. https://doi.org/10.1016/j.brainres.2015.02.011.

105. Funakoshi, K., Bagheri, M., Zhou, M., Suzuki, R., Abe, H., and Akashi, H. (2017). Highly sensitive and specific Alu-based quantification of human cells among rodent cells. Sci. Rep. *7*, 13202. https://doi.org/10.1038/s41598-017-13402-3.

**OMTM, Volume *30***

## Supplemental information

# iPSC-derived mesenchymal stem cells attenuate cerebral ischemia-reperfusion injury by inhibiting inflammatory signaling and oxidative stress

**Masafumi Arakawa, Yuki Sakamoto, Yoshitaka Miyagawa, Chikako Nito, Shiro Takahashi, Yuko Nitahara-Kasahara, Satoshi Suda, Yoshiyuki Yamazaki, Mashito Sakai, Kazumi Kimura, and Takashi Okada**

**Supplemental Materials**

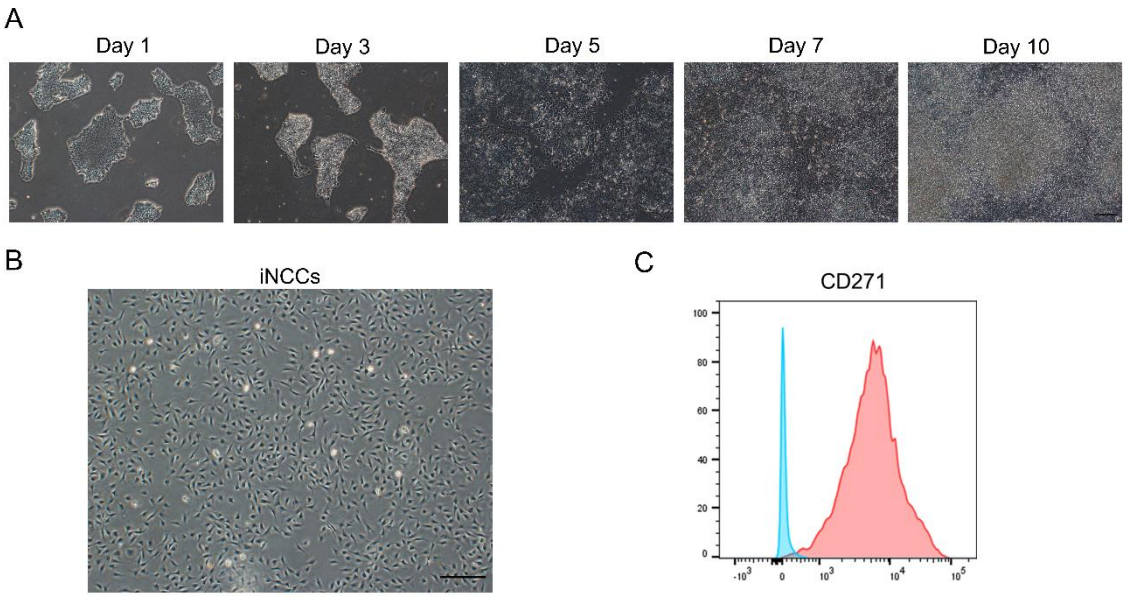


**Figure S1. Morphological changes in the induction of iPSCs to iNCCs and characterization of iNCCs**

(**A**) Morphological changes of iPSCs during iNCC differentiation (Days 1, 3, 5, 7, and 10.) Scale bar = 200 μm. (**B**) Cell morphology of iNCCs. Scale bar = 200 μm. (**C**) Surface marker analyses of iNCCs using flow cytometry. The blue histogram represents the isotype control and the red overlay represents each antigen. NCC positive marker CD271 was measured.

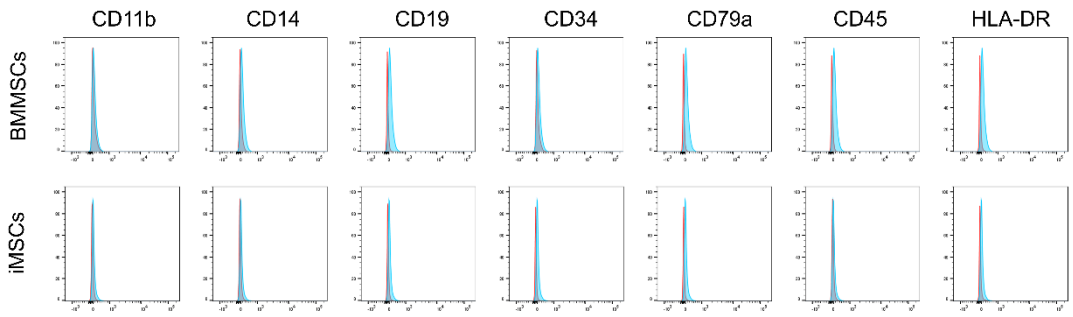


**Figure S2. Surface marker analyses of BMMSCs and iMSCs**

Surface marker analyses of BMMSCs (top) and iMSCs (bottom) using flow cytometry. The blue histogram represents the isotype control and the red overlay represents each antigen. MSC negative markers CD45, CD34, CD19, CD14, CD11b, CD79a, and HLA-DR were measured.

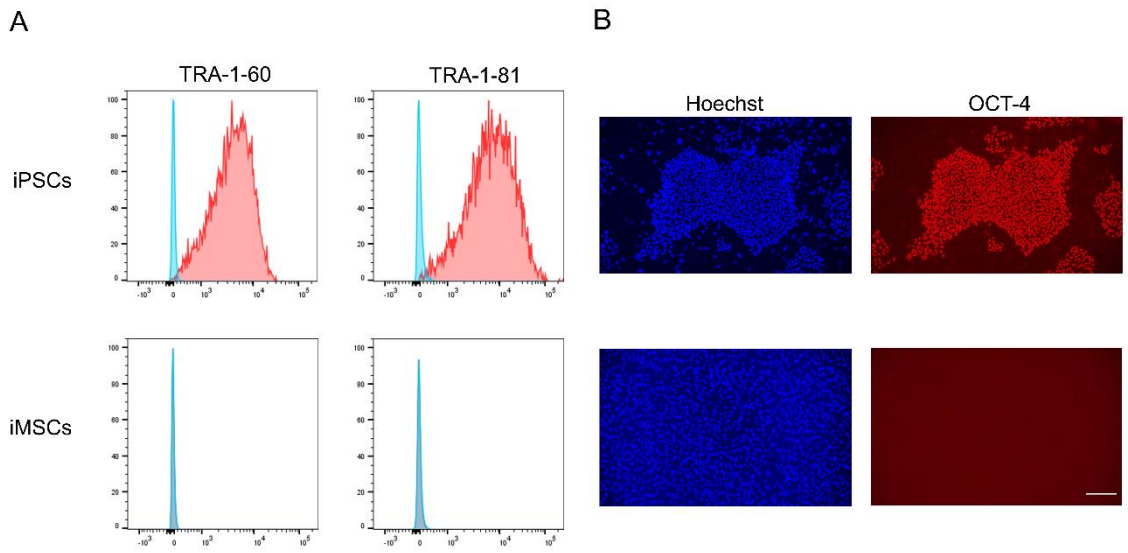


**Figure S3. Surface and intracellular marker analyses of iPSCs and iMSCs**

(**A**) Surface marker analysis of the pluripotency markers TRA-1-60 and TRA-1-81 in iPSCs and iMSCs using flow cytometry. The expression of TRA-1-60 (left) and TRA-1-81 (right) in iPSCs (top) and iMSCs (bottom) is shown. (**B**) Oct4 expression was confirmed by immunostaining. Hoechst (left) and Oct4 staining (right) of iPSCs (top) and iMSCs (bottom) are shown. Scale bar = 200 μm.

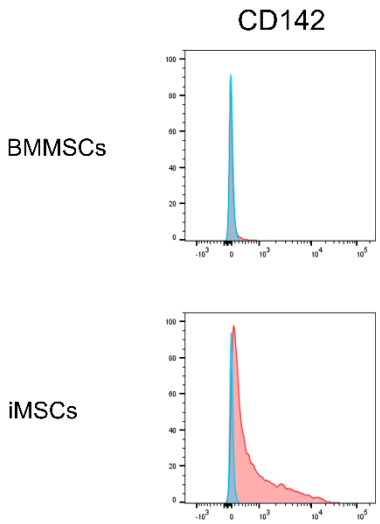


**Figure S4. Evaluation of CD142 expression in BMMSCs and iMSCs**

Surface marker analysis of BMMSCs and iMSCs using flow cytometry. The blue histogram represents the isotype control and the red overlay represents each antigen. Surface marker analysis of CD142 in BMMSCs (top) and iMSCs (bottom).

A

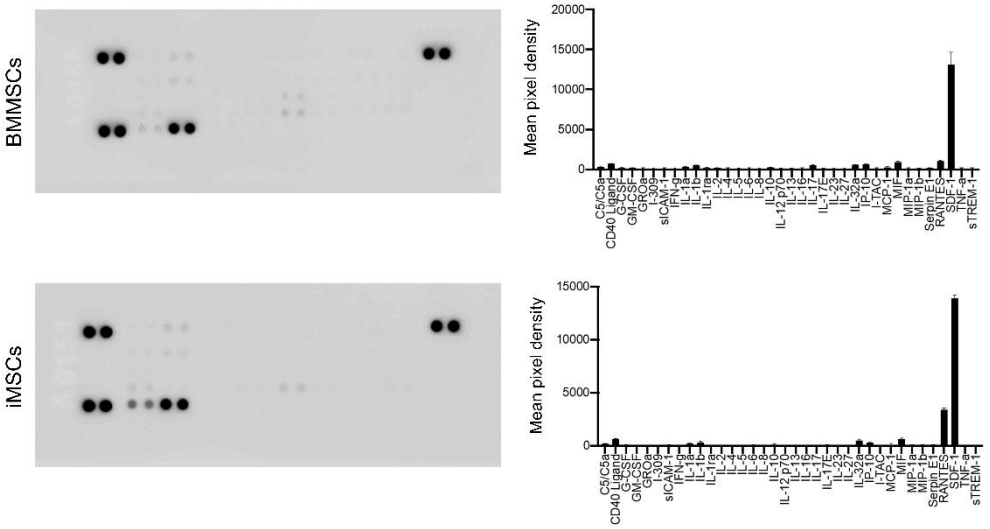
BMMSCs
iMSCs
Mean pixel density
20000
15000
10000
5000
0
C5/C5a
CD40 Ligand
G-CSF
GM-CSF
GRO
GRO-a/b/g
I-309
sICAM-1
IFN-g
IL-1a
IL-1b
IL-1ra
IL-2
IL-4
IL-5
IL-6
IL-8
IL-10
IL-12 p70
IL-13
IL-15
IL-17
IL-17E
IL-23
IL-27
IL-32a
IP-10
I-TAC
MCP-1
MIF
MIP-1a
MIP-1b
Serpin E1
RANTES
SDF-1
TNF-a
sTREM-1

B

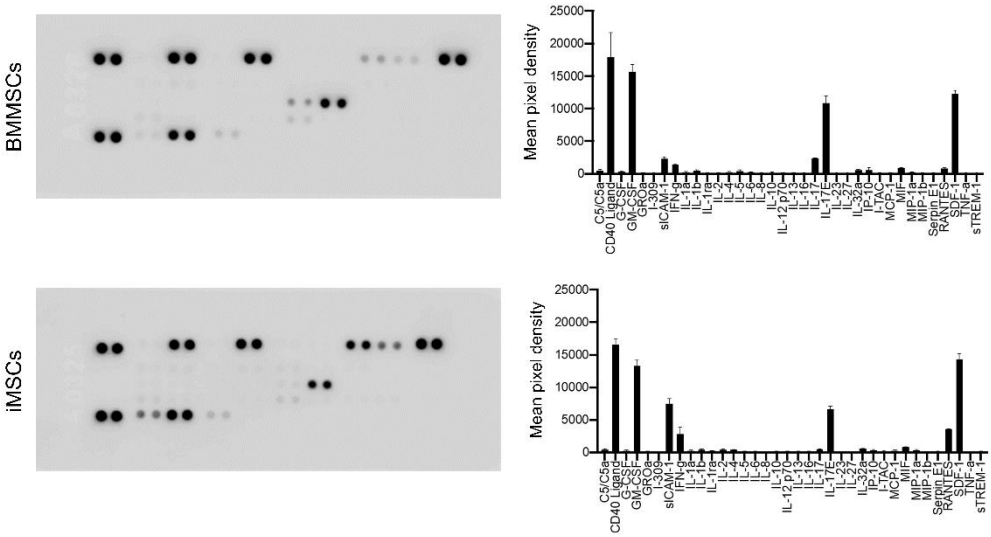
BMMSCs
iMSCs
Mean pixel density
25000
20000
15000
10000
5000
0
C5/C5a
CD40 Ligand
G-CSF
GM-CSF
GRO
GRO-a/b/g
I-309
sICAM-1
IFN-g
IL-1a
IL-1b
IL-1ra
IL-2
IL-4
IL-5
IL-6
IL-8
IL-10
IL-12 p70
IL-13
IL-15
IL-17
IL-17E
IL-23
IL-27
IL-32a
IP-10
I-TAC
MCP-1
MIF
MIP-1a
MIP-1b
Serpin E1
RANTES
SDF-1
TNF-a
sTREM-1

C

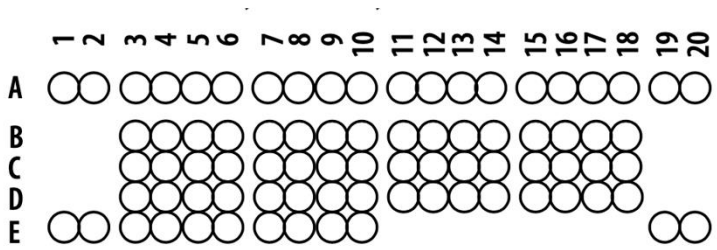
1 2 3 4 5 6 7 8 9 10 11 12 13 14 15 16 17 18 19 20
A
B
C
D
E

**Figure S5. Comparison of secreted factors in BMMSCs and iMSCs**

Cytokine array analysis of multiple cytokines secreted from BMMSCs (upper) and iMSCs (lower) with (B) or without (A) treatment with 10 ng/μL of TNF-α. The left panels show representative images of cytokine arrays, and the right panels show the profile of cytokine expression. Because cells were stimulated with TNF-α, data on TNF-α was excluded from the profiles of each cytokine array in Figure (B). (C) Coordinates of cytokine array panel. The cytokines corresponding to the coordinates are listed in Table S1.

A

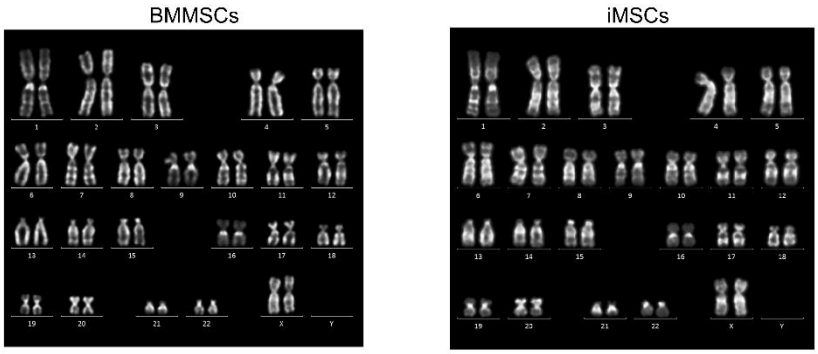


B

| | Chromosome number | | Counted nucleus | Modal No. | 4n nucleus | Modal karyotype |
|---|---|---|---|---|---|---|
| | 45 | 46 | | | | |
| BMMSCs | 2 | 18 | 20 | 46 | 1/50 (2%) | 46,XX |
| iMSCs | 2 | 18 | 20 | 46 | 6/50 (12%) | 46,XX |

**Figure S6. BMMSCs and iMSCs karyotyping analysis**

**(A)** Representative Q-band analysis results for BMMSCs (left) and iMSCs (right). Most clones showed normal karyotypes. **(B)** Summary of the karyotype analysis. The chromosome number was counted for 20 nuclei, and the tetraploid (4n) nucleus was counted for 50 nuclei for each sample.

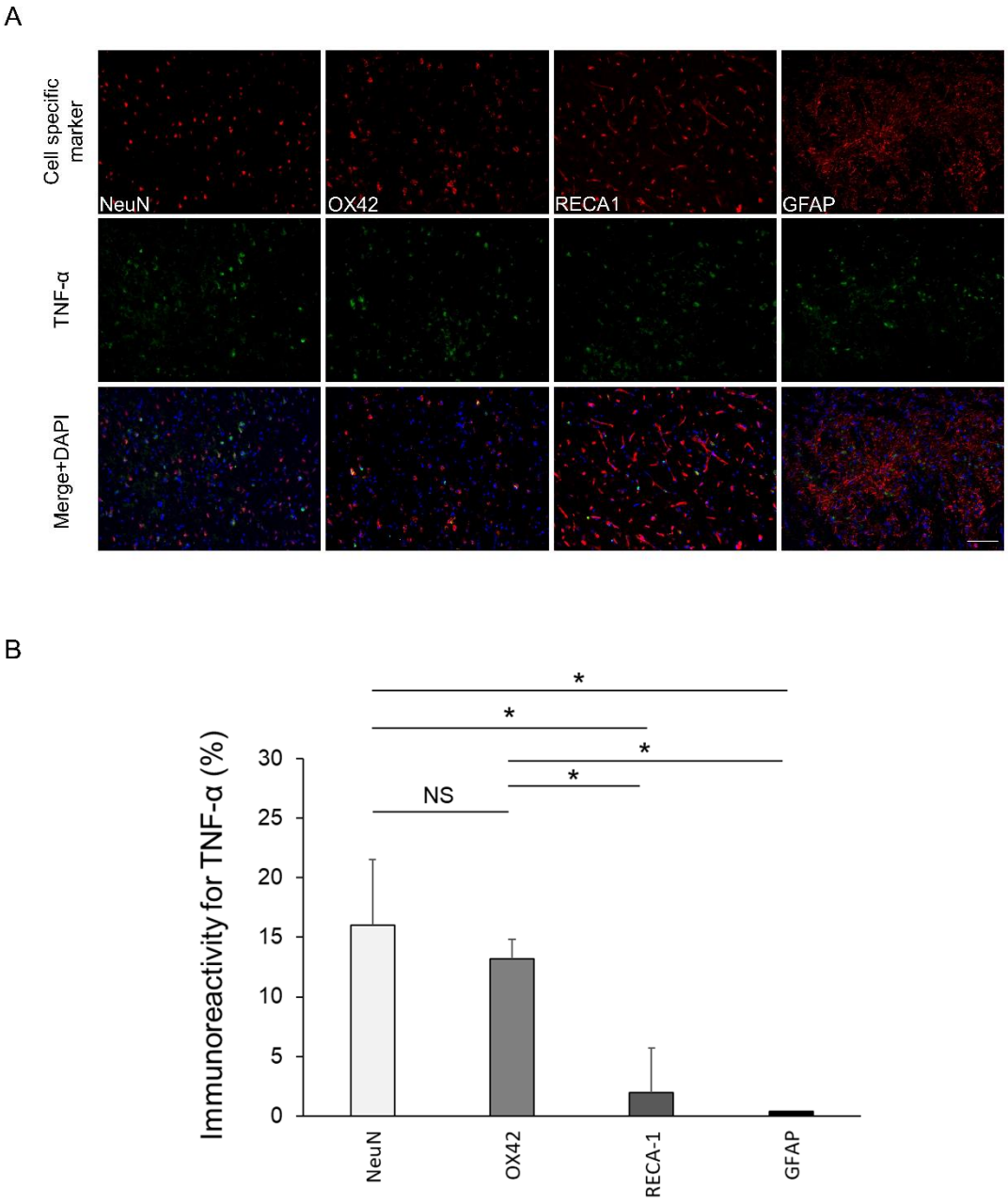


**Figure S7. Identification of TNF-α positive cells in the ischemic side of the brain**

**(A)** Immunostaining of neuron ($NeuN^+$, leftmost vertical column, red), microglial cells ($OX42^+$, second vertical column from left, red), endothelial cells ($RECA\text{-}1^+$, third vertical column from left, red), and astrocytes ($GFAP^+$, rightmost vertical column, red) in rat brain

sections. Rat brain sections were also immunostained with TNF-α (middle panels, green). Nuclei were stained in blue with DAPI. Merge overlays of three fluorescence images are shown in the bottom row. Scale bar = 100 μm. **(B)** Percentage of TNF-$\alpha^+$ cells in the field of view (*$p < 0.01$; $NeuN^+$; n = 5, $OX42^+$; n=4, RECA-$1^+$; n=5, $GFAP^+$; n=4). NS, not significant.

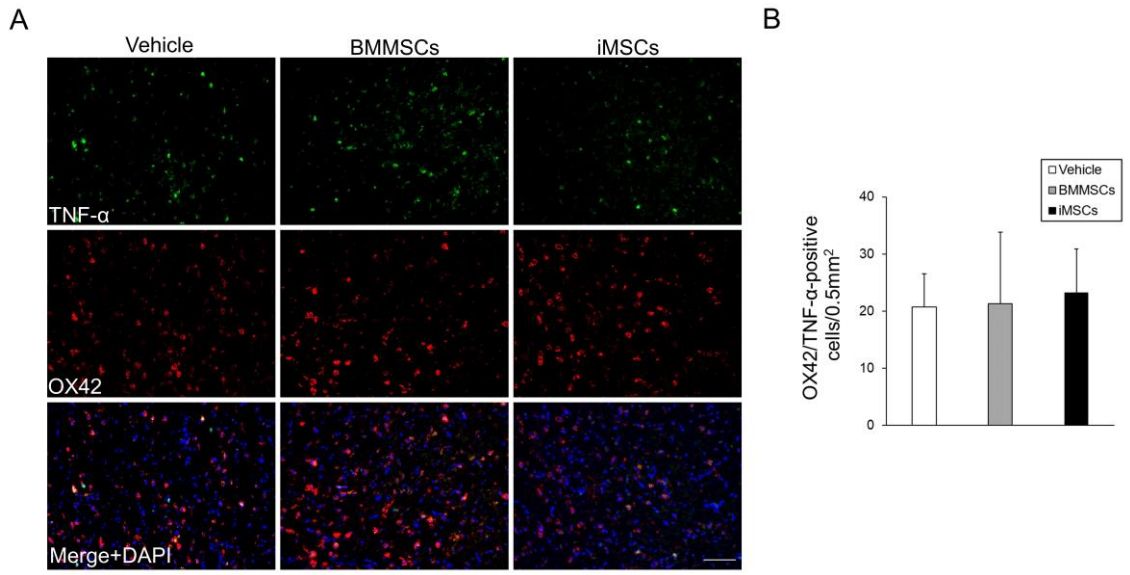


**Figure S8. Identification of OX-42/TNF-α double-positive cells in rat brain**

**(A)** Immunostaining of $OX42^{+}$ microglial cells (middle panels, red) with TNF-α (top panels, green) in rat brain sections treated with vehicle (left vertical column), BMMSCs (middle vertical column), and iMSCs (right vertical column). Nuclei were stained in blue with DAPI. Merge overlays of three fluorescence images are shown in the bottom row. Scale bar = 100 μm **(B)** Comparison of OX42/TNF-α-double-positive cells in the vehicle, BMMSC, and iMSC groups (n = 4 for each group).

Table S1. List of cytokine probes corresponding to the panel coordinates of the cytokine array

| Coordinate | Target (Alternative name) or Control | Full name |
|---|---|---|
| A1, A2 | Reference Spot | |
| A3, A4 | C5/C5a | Complement component 5/5a |
| A5, A6 | CD40ligand | Cluster of differentiation 40 |
| A7, A8 | G-CSF | Granulocyte colony-stimulating factor |
| A9, A10 | GM-CSF | Granulocyte macrophage colony-stimulating factor |
| A11, A12 | GROa | Growth-related oncogene a |
| A13, A14 | I-309 (CCL1) | C-C Motif chemokine ligand 1 |
| A15, A16 | sICAM-1 | soluble intercellular adhesion molecule-1 |
| A17, A18 | IFN-γ | Interferon-gamma |
| A19, A20 | Reference Spot | |
| B3, B4 | IL-1α | Interleukin-1alpha |
| B5, B6 | IL-1β | Interleukin-1beta |
| B7, B8 | IL-1ra | Interleukin 1 receptor antagonist |
| B9, B10 | IL-2 | Interleukin-2 |
| B11, B12 | IL-4 | Interleukin-4 |
| B13, B14 | IL-5 | Interleukin-5 |
| B15, B16 | IL-6 | Interleukin-6 |
| B17, B18 | IL-8 | Interleukin-8 |
| C3, C4 | IL-10 | Interleukin-10 |
| C5, C6 | IL-12p70 | Interleukin 12A and 12B |
| C7, C8 | IL-13 | Interleukin-13 |
| C9, C10 | IL-16 | Interleukin-16 |
| C11, C12 | IL-17 | Interleukin-17 |
| C13, C14 | IL-17E | Interleukin-17E |
| C15, C16 | IL-23 | Interleukin-23 |
| C17, C18 | IL-27 | Interleukin-27 |
| D3, D4 | IL-32α | Interleukin-32alfa |
| D5, D6 | IP-10 (CXCL10) | Interferon-gamma inducible protein 10kDa (C-X-C motif chemokine 10) |
| D7, D8 | I-TAC (CXCL11) | IFN-inducible T-cell alpha |

| | | |
|---|---|---|
| | | chemoattractant (C-X-C motif chemokine 11) |
| D9, D10 | MCP-1 (CCL2) | Monocyte chemoattractant protein-1 (C-C Motif Chemokine Ligand 2) |
| D11, D12 | MiF | Mesoderm-inducing factor |
| D13, D14 | MIP-1α (CCL3) | Macrophage inflammatory protein-1alfa (C-C Motif Chemokine Ligand 3) |
| D15, D16 | MIP-1β (CCL4) | Macrophage inflammatory protein-1beta (C-C Motif Chemokine Ligand 4) |
| D17, D18 | Serpin E1/PAI-1 | Plasminogen activator inhibitor type 1 |
| E1, E2 | Reference Spot | |
| E3, E4 | RANTES | Regulated on activation, normal T cell expressed and presumably secreted |
| E5, E6 | SDF-1 (CXCL12) | Stromal cell-derived factor 1 (C-X-C motif chemokine 12) |
| E7, E8 | TNF-α | Tumor necrosis factor-alfa |
| E9, E10 | sTREM-1 | Soluble factor triggering receptor Expressed on myeloid cells-1 |
| E19, E20 | Negative Control | |